The Paleocene Eocene Thermal Maximum in the Hanna Basin, WY: Constraints from Organic Carbon Isotopes and Palynological Data

Caroline Pew

A thesis submitted in partial fulfillment of the requirements for the degree of

Master of Science

University of Washington

2013

Committee:

Roger Buick

Caroline Stromberg

Program Authorized to Offer Degree:

Earth and Space Sciences

Abstract

The P-E boundary, approximately 56 Ma, coincides with a global climatic event, the Paleocene-Eocene Thermal Maximum (PETM). The PETM is believed to have resulted from a 2-8 fold increase in atmospheric pCO_2 in less than 10,000 years, which resulted in increased temperatures of 5-8°C globally. The PETM is an event of great interest as it is believed to be the best ancient analogue for modern climate change.

This study aims to more precisely pinpoint the stratigraphic location of the PETM in the Hanna Formation in the Hanna Basin, WY. Previous studies have identified the late Paleocene at 2350 meters above the base of the section and the early Eocene as 2800 meters above the base of the section. In order to accomplish this, organic carbon isotopes from carbonaceous shales and coal deposits were measured in order to establish the presence of the characteristic CIE associated with the PETM and the P-E. Palynological samples were also extracted from carbonaceous shales and coals in order to determine the presence of the index pollen, which were used as biostratigraphic markers to determine the exact placement of the P-E boundary within the section. Additionally, pollen abundance and occurrence were determined throughout the section in order to see if the palynological record suggests paleoecological changes associated with warming at the PETM.

Results show an approximately -2 ‰ shift in organic carbon isotopic signature between approximately 2600-2650 meters above the base of the Hanna Formation. *Platycarya platycaryoides* pollen first occurs just down section of the observed CIE in organic carbon, first appearing at 2540 meters above the base of the section. The first occurrence of *Platycarya platycaryoides* near the observed carbon isotope excursion suggests that the onset of the PETM

and the P-E boundary in the Hanna Basin are located between 2540 and 2650 meters. Thus, this study succeeded in more precisely locating the PETM with in the Hanna Formation. Moreover, this study shows that the Hanna Basin records the PETM event over a greater thickness of section with higher stratigraphic resolution than adjacent basins with a disjunct first occurrence of P-E indicator palynomorphs and the characteristic negative carbon isotope excursion of the PETM. Thus the Hanna Basin reveals greater biogeochemical complexity than other adjacent basins and suggests that either local factors such as old heavy carbon erosion, early floral immigration or changing environmental circumstances complicated the local record, or that greater stratigraphic resolution indicates that biotic change and carbon cycle shifts were not coincident. If the latter, then rapid climatic warming may have post-dated major biological perturbations, which has implications for modern global warming.

Dedication

I would like to dedicate this thesis to my family and friends for their unwavering support. To my mother who read all my drafts of every research grant proposal I say thank you for helping me find my voice and for just being there. To my mother, my father and my nephew, Gabriel, thank you for sharing time in the field with me and carrying me through trying times out there in the wilds of Wyoming. Carrying me through being covered in ticks, being lost on two tracks and fusing my engine on a Sunday in the middle of nowhere. To my friends – particularly - Liz, Heidi, Drie and Kellie who believed in me and encouraged me to go on even when I felt like throwing in the towel – I would certainly never have finished without each of you.

And finally, to my wife, Jillanna…

You have been my strength

You have carried me through hard times

The love of my life

Thank you to everyone who helped play a part in forming this thesis.

With relief and gratitude,

Caroline Rose Pew

Table of Contents

Introduction

1.1 The Paleocene Eocene Thermal Maximum (PETM)

The PETM (Paleocene-Eocene Thermal Maximum) was a paleoclimate event recorded in both terrestrial and marine records. It was a rapid global warming event of similar magnitude to projected modern climate change (Wing *et al*., 2005). As with modern climate change the PETM is also thought to have been caused by a geologically short term (~10kyr) increased flux of carbon to the atmosphere (Pagani *et al*., 2006a; McInerney & Wing, 2011). The rapid influx of carbon is most often attributed to a large scale methane hydrate release, so the PETM is believed to have been precipitated by an initial warming period or other destabilization mechanism (Storey *et al*., 2007).

Methane hydrates are methane molecules entrapped in frozen water molecules. These often form in reducing environments where there are high rates of organic sedimentation such as the continental slope (Dickens *et al*., 1995). Methane hydrates can be destabilized by changes in temperature, sea-level and ocean circulation (Dickens *et al*., 1995, 1997). Continental slope failure can also decrease the pressure on methane hydrates by removing overlying sediment also resulting in dissociation of methane hydrates (Katz *et al*., 1999).

Since methane readily oxidizes to CO_2 in an oxygenated ocean and atmosphere, it is safe to assume that most of the methane released during the PETM was converted to CO_2 in a geologic instant (Jacob, 1999). The result was a 2-8 fold increase in atmospheric pCO_2 in less than 10,000 years (Cramer & Kent, 2005; Pagani *et al*., 2006a). This is commensurate to the projected 2-3 fold increase in atmospheric pCO_2 by 2100 in the modern atmosphere (IPCC, 2007). Therefore, studying the paleoclimatic and paleoecological effects of the PETM could provide valuable

insight into the future effects of modern climate change. As many scientists have suggested that anthropogenic warming could directly lead to conditions similar to those experienced at the PETM, it is vitally important to study this past event of climate change (Wing *et al*., 2005).

The Hanna Basin, WY contains an as yet poorly studied terrestrial section spanning the P-E Boundary with a rich stratigraphic record (Lillegraven *et al*., 2004). Composed dominantly of organic-rich floodplain and fine-grained alluvial fan deposits, this section has ideal facies for fossil plant preservation. Formed during the Laramide Orogeny, the Hanna Basin is the result of uplift and erosion of mountains of the Sweetwater Arch (Higgins, 2003; Lillegraven & Snoke, 1996). This rapid uplift and erosion led to high rates of sedimentation, allowing high stratigraphic resolution.

Consequently, though the PETM has been studied in other terrestrial sections such as the Powder River Basin and Bighorn Basin, the Hanna Basin has the potential to yield more complete and higher resolution paleoecological and isotopic data. However, due to the inconsistent preservation of animal (in particular vertebrate) fossils, the precise stratigraphic position of the P-E boundary is unknown, and must be located using palynological techniques and isotopic chemostratigraphy (Lillegraven *et al*., 2004). This thesis attempts to do just that.

1.2 How Terrestrial Organic Carbon Isotopes Were Affected during the PETM

Globally, the PETM is marked in terrestrial and marine environments by a negative carbon isotope excursion (CIE) (Luterbacher *et al*., 2000). Mean values of the CIE differ with terrestrial sections showing a mean shift of −4.7±1.5‰ in $\delta^{13}C$ and marine sections exhibiting a −2.8±1.3‰ shift (McInerney & Wing, 2011). Marine and terrestrial organic carbon sources were

shown to have intermediate values, marine carbonates showed the lowest values while terrestrial plant lipids and carbonates showed the highest values (McInerney and Wing, 2011).

Derived primarily from plant material, the terrestrial organic carbon record reflects the isotopic composition of the paleoatmosphere, offset by a known fractionation that occurs during photosynthesis. Therefore, the known fractionation can be used to calculate the atmospheric carbon isotope composition at that time. In addition, estimates of the amount of carbon necessary to create a 2-5‰ shift globally can be made based on assumptions of the isotopic composition of the carbon source to the atmosphere during the PETM.

Methane hydrates are the most commonly invoked source for the carbon release during the PETM, which caused the observed CIE during this event. This is largely due to the fact that in order to create a global shift in carbon isotopes of negative 2-5‰ the source of carbon released would have to be large in volume and a have a very negative value. Methane hydrates have approximately a -60‰ average isotopic composition, so this coupled with the potentially large size of the methane hydrate reservoir (>1500 Gtons) make it plausible that methane hydrates were a major contributor to the observed CIE during the PETM (McInerney and Wing, 2011; Kvenvolden, 1999).

Methane hydrates alone may be insufficient to account for the rapid warming and CIE at the P-E boundary, based on Intergovernmental Panel on Climate Change estimates of CO_2 climate sensitivity of 2.5°C per doubling of CO_2 (IPCC, 2007; Kvenvolden, 1999). Hence, some other sources of carbon may have contributed to the warming during the PETM.

Oxidation of large amounts of organic carbon through the burning of pre-existing peats and coals (Kurtz et al., 2003) may have added carbon dioxide to the P-E atmosphere. This is

postulated to have been caused by a combination of dryer climates, increased atmospheric oxygenation and tectonic uplift of coal deposits (Kurtz *et al*., 2003). However, this is not a likely scenario due to the fact that the $\delta^{13}C$ of peat and coal is approximately −22‰ (McInerney & Wing, 2011), insufficiently isotopically light to have much effect on atmospheric $\delta^{13}C$ without the addition of vast quantities. Notably, there doesn't appear to be evidence for a substantial increase of large scale byproducts of organic material combustion in global ocean basins and there is no statistically significant increase in black carbon and other combustion products (Moore & Kurtz, 2008).

Peat may also have contributed to the observed CIE at the onset of the PETM through oxidation due to melting permafrost at high latitudes (DeConto *et al*., 2010). Although there is no evidence for Antarctica having an ice cap during the Paleocene-Eocene time period, there was potentially permafrost, which would have prevented organic material from oxidizing. If the permafrost rapidly melted due to an initial warming event, it would have allowed the organic material to become oxidized, releasing carbon to the atmosphere (DeConto *et al*., 2010). The $\delta^{13}C$ of this organic material is estimated at −30‰, also insufficient on its own to account for the observed CIE (McInerney & Wing, 2011).

However, there was also the North Atlantic Igneous Province (NAIP) opening at this time, which intruded into and caused metamorphic degassing of organic-rich Cretaceous/ Paleocene mudstones in the North Atlantic (Svensen *et al*., 2004, 2010; Westerhold *et al*., 2009). The average $\delta^{13}C$of these sediments is estimated at −30‰, which too would be insufficient to account for the global magnitude of the observed CIE (McInerney & Wing, 2011).

Large epicontinental seaways existed in the Cretaceous and Paleocene, such as the Western Interior Seaway in North America and large areas of central Asia are known to have had shallow seas present during the Paleocene and Eocene (Gavrilov *et al*., 2003). The desiccation and oxidative weathering of the organic material left behind by these large epicontinental seaways as they became tectonically isolated from the ocean could have contributed carbon to the atmosphere with a $\delta^{13}C$ estimated at −22‰ (Higgins & Schrag, 2006). Again, this source would be insufficiently negative and insufficiently large to account for the magnitude of the globally observed CIE (McInerney & Wing, 2011). Additionally, there doesn't appear to be a large epicontinental seaway which dried up during the PETM interval (Gavrilov *et al*., 2003).

Therefore, given the evidence, it is likely that methane hydrates, derived from microbial activity, with a $\delta^{13}C$ estimated at −60‰ would have been the only source negative enough and large enough to create the observed CIE at the onset of the PETM by itself (McInerney & Wing, 2011; Kvenvolden, 1999). However, it is probable that these other sources contributed to and exacerbated the CIE and subsequent warming at the PETM.

1.3 Previous Work on the Stratigraphic Location of the PETM in the Hanna Basin, WY

The largest challenge in locating the P-E boundary and thus the PETM in the Hanna Basin is the lack of material suitable for chronostratigraphy. There are, as yet, no ash layers known in the area which could be used for radiometric dating. There are no igneous rocks which could be used for dating using paleomagnetism. Thus it falls to chemostratigraphy and biostratigraphy as the primary ways to assign age brackets and correlate the Hanna Formation with other PETM sections. Unfortunately, in large portions of the succession, there is a complete

lack of vertebrate fossil preservation, unlike other adjacent P-E boundary sections. Therefore, the previous attempts to constrain the P-E boundary in the Hanna Basin have utilized other tools.

Fresh water mollusks were used in a study by Kirschner (1984). Late Paleocene species were found at approximately 2350 meters above the base of the Hanna Formation. A very limited palynological study of the Hanna Formation yielded a first occurrence of *Platycarya platycaryoides*, an indicator species of the early Eocene in North America (Lillegraven *et al*., 2004; Nichols & Ott, 1978), at approximately 2800 meters above the base of the Hanna Formation. However, this previous study involved examination of fewer than 10 samples over the entirety of the 3000 meter Hanna Formation, so it only narrowed down the location of the P-E boundary to a 600 meter stratigraphic range. This is why that section of the Hanna Formation – between 2300 meters and 2900 meters- became the focus of the study reported in this thesis.

1.4 Objectives of this Thesis

This study aims to establish the stratigraphic location of the PETM in the Hanna Formation in the Hanna Basin, WY. Organic carbon isotopes from carbonaceous shales and coal deposits were measured using a continuous flow mass spectrometer in order to establish the presence of the characteristic CIE associated with the PETM and the P-E boundary in terrestrial sediments. Palynological samples were also prepared from carbonaceous shales and coals in order to determine the presence of the index pollen *Platycarya*, which is an indicator of the earliest Eocene palynozone E-1 of Nichols and Ott (1978). This is equivalent to the *Platycarya platycaryoides* Zone of Pocknall (1987) and Zone Z of Tschudy (1976). *Platycarya* therefore acts as a biostratigraphic constraint on the exact placement of the P-E boundary within the section. Additionally, palynomorph distributions and abundances were determined throughout

the section in order to see if the palynological record shows paleoecological changes associated with warming at the PETM.

Chapter 2: The Paleocene- Eocene Thermal Maximum: Biological and Climatic Events

2.1 History of the PETM

The earliest comprehensive account of the PETM, linking isotopic excursions and biotic changes with rapid global warming, was by Kennett and Stott (1991). Initially the PETM was most commonly referred to as the Late Paleocene Thermal Maximum (LPTM) or sometimes the Initial Eocene Thermal Maximum (IETM) (McInerney & Wing, 2011). Kennett & Stott 1991 noted that there was a carbon isotope excursion in foraminiferal shells of -2‰ in benthic species and -4‰ in planktonic forms in Arctic deep ocean drill cores. This was concurrent with a 3-4°C increase in sea surface temperatures in sea surface temperatures as estimated from $\delta^{18}O$ of foraminiferal carbonates (Kennett & Stott, 1991). These changes were contemporaneous with a benthic foraminiferal mass extinction event whereas planktonic species at the same sites were unaffected (Bralower, 2002; Koch *et al*., 1992; Thomas, 1989). The differential response in benthic and planktonic foraminifera was commonly attributed to increased bottom water temperatures and shoaling of the lysocline (Bralower, 1997, 2002; Giusberti, 2007). This finding was rapidly replicated elsewhere and shown to be global, spurring a large amount of research into the cause of this difference in benthic and planktonic response to the PETM (Bains, 1999; Bralower, 2002; Gibbs, 2006).

Koch *et al*. (1992) attempted to link the observed negative CIE at the onset of the PETM in marine sediments with the CIE in terrestrial soil carbonate nodules in order to establish that this was a global event affecting both terrestrial and marine environments. The study found that there was a CIE in both marine sediments and soil carbonate nodules. Terrestrial sediments show a negative carbon isotope excursion which is sometimes larger, typically 2-5‰ depending on the

source setting, than in marine sections which generally show a 2-3‰ shift in $\delta^{13}C$ values (Pagani *et al*., 2006a; Giusberti, 2007; Koch *et al*., 1992). Increased carbon isotope discrimination in plants due to increasing moisture availability has been invoked as a potential cause for the larger CIE observed in terrestrial systems (Bowen *et al*., 2004). The CIE has become such an important marker of the PETM, and thus the P-E Boundary, that it is now used as a method to correlate between marine and terrestrial PETM sections (Gingerich, 2006).

The Koch *et al*.(1992) study was also one of the first to estimate pCO_2 levels during the PETM, which were initially determined to be >750 ppm. Later studies would find this to be a rather modest estimate of pCO_2 change, with evidence for a 2-8 fold increase in pCO_2 upon background levels of approximately 200-300ppm (Zachos, 2003; Cramer *et al*., 2005).

Corfield (1994) conducted a large scale study of Cenozoic $\delta^{13}C$ values in marine settings. It was noted that $\delta^{13}C$ of bulk marine carbonates decreased on the order of -2‰ during the post K/Pg recovery interval at the start of the Cenozoic as a side effect of low productivity resulting from mass extinctions at the K/Pg boundary (Corfield, 1994; Zachos *et al*., 2001). As the Cenozoic progressed $\delta^{13}C$ values increased, returning to pre-K/Pg values. This was largely attributed to recovery of productivity after the K/T mass extinction, which led to increased sequestration and burial of organic carbon (Corfield, 1994). Going into the latest Paleocene $\delta^{13}C$ values were already beginning to decrease, but then there was an exponential decrease concurrent with the P-E boundary of 2-5 ‰ in terrestrial and 2-3‰ in marine settings (Corfield, 1994; Zachos *et al*., 2001).

The widespread presence of the negative CIE found by Corfield sparked interest from a number of other researchers. Dickens *et al*. (1995) investigated a number of potential causes for

the PETM, including the possibility that glacial/interglacial biomass transfer to the deep ocean reservoir or that volcanic outgassing may have accounted for the negative CIE. Both of these were discounted on the basis that the reservoir sizes were too small and/or the source had an insufficiently negative $\delta^{13}C$ value to account for the observed negative CIE (Dickens *et al*., 1995).

Dickens *et al*. (1995) also introduced the idea that deep water warming could have caused dissociation of methane hydrate deposits in deep marine sediments (see figure 2.1). The initial warming would have driven the hydrates out of their stability zone, precipitating a large scale dissociation event. In a geologic instant gigatons of methane would have been released to the ocean and atmosphere. Methane readily oxidizes in Earth's oxic environment to CO_2 through a series of reactions with free radicals in the atmosphere. In the modern atmosphere the residence time of methane is 10 years, but with such a large amount of methane being released in a short period of time this residence time would have likely been longer during the PETM (IPCC, 2007; Bralower, 1997). However, once the methane was released to the atmosphere and oxidized to CO_2, it would have readily been taken up by plants, dissolved in ocean water and incorporated into the shells of carbonate-shelled marine organisms. Since methane has a highly negative $\delta^{13}C$ value, averaging -50‰ but if from microbial sources as light as -60‰, a massive input of methane-derived carbon was thought to be a viable potential source for the CIE associated with the onset of the PETM (Kvenvolden, 1999). However, it was still unclear if P-E methane hydrate reservoirs were large enough to produce the observed CIE. Early estimates predicted that at least 1500 Gt of methane would have to have been released in order to produce the CIE (Bains *et al*., 1999). However, more recent modeling results suggest that 4600 Gt of methane clathrates would have to have been released in order to create the observed CIE (Diefendorf *et al*., 2010).

Other factors that may have contributed to carbon release result from the tectonic environment at the P-E Boundary. During that time the North Atlantic Igneous Province (NAIP) was very active, due to the opening of the Atlantic Ocean Basin (Storey *et al*., 2007). The NAIP would have directly contributed slightly isotopically light carbon to the atmosphere during degassing. Additionally, the NAIP volcanics came into contact with many organic rich marine sediments. These sediments, when heated by magma from the NAIP, would have be subjected to organic material combustion, adding another potential source for providing carbon dioxide to the atmosphere (Varekamp *et al*., 1992; Storey *et al*., 2007)

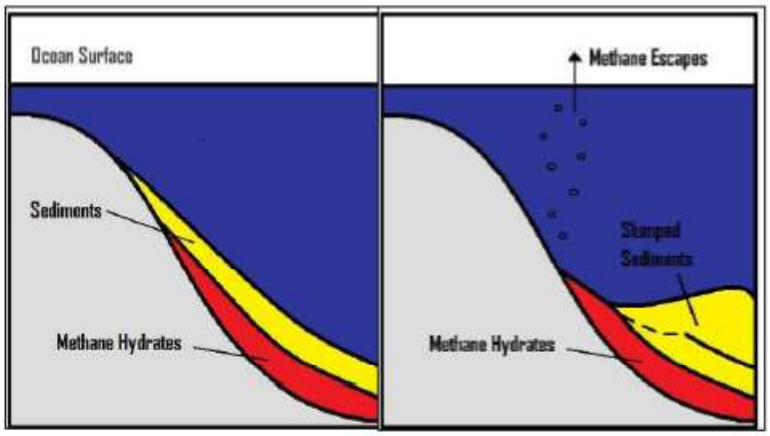

Figure 2.1 Methane hydrates build up in continental slope sediments, when they are destabilized methane hydrates dissociate, causing subsidence and release to the atmosphere.

During the Cretaceous, active seafloor spreading margins increased buoyancy of the oceanic plates, thus displacing water from the ocean basins (Seton *et al*., 2009). Additionally, there were no known polar ice caps at this time, which also contributed to global sea level being

high during the Cretaceous (Sickel *et al*., 2004; Storey *et al*., 2007). High sea level led to the creation of epicontinental seaways, some of which were sequestered from the ocean by isostatic rebound and tectonic uplift (Higgins & Schrag, 2006). During the PETM interval overall seafloor spreading rates had slowed, decreasing oceanic crust buoyancy and resulting in a decrease in sealevel to approximately 300 meters below modern (Haq *et al*., 1988). These large epicontinental seaways that formed during the Cretaceous eventually desiccated, so once organic material within them became exposed to the atmosphere, it reacted with oxygen which would have also contributed to the release of isotopically light carbon dioxide to the atmosphere (Higgins & Schrag, 2006).

Biomass burning, with a possible cometary impact trigger mechanism, has also been invoked as a potential cause for the PETM (Moore & Kurtz, 2008; Kent *et al*., 2003). The evidence for this was a thin iridium layer with graphitic black carbon found in some PETM sections. The graphitic black carbon had the same $\delta^{13}C$ as the CIE, indicating that the material burned was living at the time of the PETM and not burnt fossil plant material, such as peat or lignite. However, these hypotheses were largely refuted on the basis that the iridium layer was very low in concentration and the graphitic black carbon was insufficient in quantity to account for the CIE (Moore & Kurtz, 2008; Kent *et al*., 2003)

The methane hydrate dissociation hypothesis has thus become the most widely accepted cause for the PETM. However, some investigators have questioned whether the assumptions of methane hydrate reservoir size and release rate were viable (Zeebe *et al*., 2009; Cramer & Kent, 2005). Later estimates of methane release increased the minimum volume necessary to produce the CIE to >2000 Gt (Giusberti *et al*., 2007; Diefendorf *et al*., 2010). Cramer *et al*. (2005) argued that the actual methane reservoir at the time was smaller than earlier studies predicted which

based PETM methane hydrate reservoir size on estimates of the modern reservoir. There was less continental slope area at the correct depth for methane hydrate stability during the PETM and global average temperatures were warmer, meaning fewer areas were sufficiently cold for methane hydrates to be stable prior to the onset of the PETM. In addition only an estimated 19% of the methane released was likely to actually exit the methane hydrate stability zone without being locally reconsumed or recrystallized and redeposited (Cramer *et al*., 2005; Cramer *et al*., 2007; Panchuk, 2008).

Consequently, investigators are still exploring the many possible causes for the PETM. Although a consensus has not been reached, methane hydrate dissociation is still accepted as the most likely and largest contributing factor to the onset of the PETM.

2.2 Biological Events

The PETM is not commonly recognized as a global mass extinction event, except with respect to benthic foraminiferal species (Bains *et al*., 1999; Thomas, 1989). There was not a sudden significant extinction of land plants, mammals, marine invertebrates or planktonic foraminifera (McInerney & Wing, 2011). However, land plants did slowly transition from the late Paleocene flora to a distinct early Eocene flora with some overlap and persistence of late Paleocene species and first occurrences of many new species in North America at the P-E boundary (Harrington, 2003). Nannoplankton showed a paradoxical pattern of both increased origination and extinction across the PETM (Gibbs *et al*., 2006). In mammalian communities there were many first occurrences of new species, and dwarfism and migration were common responses in persisting mammalian species (Clyde, 1998; Peters, 2000; Gingerich, 2003)

The PETM is very different than the Big 5 mass extinctions in that the impact on organisms globally was much less, with the exception of the benthic foraminifera. The Big 5 mass extinctions all share some common characteristics. During each of those events approximately 50% or more of the genera pre-event went extinct at the event horizon. Further, during the Big 5 mass extinctions typically 60% or more of the total species on Earth went extinct (Raup, 1982). Therefore, the ecological effect of the PETM was much less devastating than during the Big 5 mass extinctions in that only one group of organisms, marine benthic foraminifera, was subject to mass extinction. However, there was a large diversification in land mammals during the PETM as well as a diversification in plant species, particularly within the Juglandaceae family (Gingerich, 2003; Clyde 1998; Nichols & Ott, 1978). The Big 5 mass extinctions also often exhibited diversification events after the initial extinction and not merely because of refilling of old niches, but also because of the opening of new niches due to climatic and environmental restructuring (Jablonski & Lindberg, 2001).

Marine ecosystems during the PETM have primarily been studied through microfossil data (Ivany & Sessa, 2010). This doesn't allow for a complete picture of trophic structures during the PETM. However, the PETM is best recognized in marine sections by the characteristic and well documented mass extinction of up to 50% of benthic foraminifera (Thomas, 1989, 2007). Studies of the rate of extinction of benthic foraminifera indicate that the extinctions were gradual rather than geologically instantaneous (Alegret *et al*., 2009a, b). This would be consistent with the proposed causes for the extinction, which include increased acidity of deep water, lower oxygen levels and higher temperatures (Thomas 2003, 2007). There is also evidence for increased marine salinity and shoaling of the carbonate compensation depth (Bralower 1997; Giusberti *et al*., 2007). It is estimated that in some areas this shoaling may have

been up to 2 km during the PETM, which would have acted as a strong selective pressure upon benthic carbonate-shelled organisms, such as foraminifera (Zachos, 2005). Benthic foraminifera may also have adversely affected by ocean stratification caused by a slowing of ocean circulation as a result of decreasing pole to equator temperature gradients (Higgins & Schrag, 2006; Luciana *et al*., 2007).

The benthic foraminifera that do persist through the PETM show thinned walls, are smaller in size than pre-PETM individuals or have agglutinated shells (Thomas, 2007). Other benthic organisms and planktonic foraminifera do not experience this same pattern of mass extinction. The only other benthic microorganisms that have been studied comprehensively across the PETM are ostracodes (Steineck & Thomas, 1996). These do not show a consistent pattern of response, but rather vary in their response locally with little change in some areas and decreasing diversity in others (Webb *et al*., 2009; Morsi *et al*., 2011).

Planktonic foraminifera did not suffer mass extinctions in the manner that benthic foraminifera did, although they did show localized decreases in abundance in tropical areas and in the open ocean perhaps due to food stress in tropical waters (Bralower, 2002; Bralower 2007; Gibbs *et al*., 2006) and some tropical species migrated to higher latitudes during the PETM interval (Thomas & Shackleton, 1996). Instead, planktonic foraminifera in general underwent speciation during the PETM (Bralower, 1997, 2002). Evolutionary changes in form occurred for planktonic foraminifera as well, as average body size increased during the PETM, possibly the result of increased capacity to host photosymbiotic bacteria in the oligotrophic conditions created by a stratified ocean (Kaiho *et al*., 1996). Interestingly, planktonic foraminifera also appear to have exhibited higher productivity during the PETM in specific areas such as continental margins (Gibbs *et al*., 2006). Evidence for increased terrestrial input to the continental margins

suggests increased weathering and erosion on the continents, leading to higher nutrient levels which in turn increased primary productivity and likely contributed to the speciation of planktonic foraminifera during this time period (Crouch *et al*., 2003). Diversity and productivity in the open ocean decreased during the peak of PETM, suggesting oligotrophic conditions, whereas shelf diversity and productivity varied locally based on nutrient availability, likely due to the local weathering, erosion and river deposition rates (Gibbs, 2006; Clechenko *et al*., 2005).

Coccolithophorids were also impacted by the PETM, although it appears to be largely genera-specific as some coccoliths showed an increase in productivity while others showed a decrease (Matell *et al*., 2005). Sr/Ca ratios, which are a proxy for productivity in coccolithophorids, increased by up to 40% after the CIE in certain genera of coccolithophorid shells (Stoll& Bains, 2003). However increased ratios indicating higher productivity were most prevalent near the continental shelf, which is consistent with increased weathering rates and nutrient fluxes. Coccolithophorid platelets show that oligotrophically adapated species became more abundant in the open ocean, while eutrophic species increased along the continental margin (Brawlower, 2002, Gibbs *et al*., 2006; Agnini *et al*., 2007; Angori *et al*., 2007). There appears to be an overall warming trend globally, illustrated by the elimination of cool water species in low latitudes concurrent with replacement of cold water species with warm water species near Antarctica (Angori *et al*., 2007; Bown & Pearson, 2009; Mutterlose *et al*., 2007). Overall global nannofossil origination and extinction rates during the PETM were the highest in the Cenozoic era (Gibbs *et al*., 2006).

In terrestrial sections the PETM is characterized by the first occurrence of several extant mammalian orders (Gingerich, 2006). Floral assemblages exhibit a short lived transitional stage where megaflora change dramatically to more thermophilic taxa in general, followed by a return

to floras similar to the late Paleocene but with a few Eocene migrants and relative abundance shifts (McInerney & Wing, 2011). There are several first occurrences of reptilian species in North America during the PETM as well, thought to be migrant species (Smith, 2009). Indirect studies of insects show that there was a marked increase in insect herbivory during the PETM (Currano *et al*., 2008).

Mammals responded to the PETM, but not with mass extinction events as with the benthic foraminifera. At this time several key modern orders of mammals, Artiodactyla, Perissodactyla and Primates (APP taxa), as well as the now extinct Hyaenodontidae, first appeared in the fossil record on all three northern continents during the PETM interval (Koch *et al*., 1992, 1995; Gingerich, 2006; Bowen *et al*., 2005). In fact, due to improved correlation of the PETM worldwide, using the characteristic CIE, it is believed that the APA taxa all appeared in the 3 northern continents within 10,000 years of each other, despite the fact that Paleocene faunas were largely continentally endemic (Gingerich, 2006; Peters, 2000; Hooker, 1998). Their appearance has been linked to diversification and dispersal in response to rapid environmental change associated with the PETM (Gingerich, 2006; Koch *et al*., 1995). Like the *P. platycaryoides* pollen that appears first in the earliest Eocene, precursors to the APP taxa have not been found in the geologic record (Gingerich, 2006). High-latitude land bridges were the most likely dispersal paths for these mammal groups, and this is supported by the presence of Hyaenodontidae in Chinese pre-PETM sections indicating that this mammal group originated in Asia and subsequently migrated to North America where it first appears at the P-E boundary (Peters, 2000; Koch *et al*., 1995; Bowen *et al*., 2002).

The initial APP taxa show smaller body sizes than their nearest descendants (Gingerich, 2006; Chester *et al*., 2010). This is consistent with the transient dwarfism of mammalian species

that persisted from the late Paleocene into the early Eocene (Clyde, 1998; Chester *et al*., 2010; Strait, 2001). This episode of dwarfism and first appearance of the APP taxa also occurred concurrently with numerous abrupt land mammal speciations (Gingerich, 2003; Clyde 1998). These are observed in a number of places, including the Big Horn Basin, WY.

While mammals in general did not suffer significant extinctions, *Plesiadapis*, a late Paleocene taxon common in both North America and Europe with morphological similarities to Proprimates, went extinct (Gingerich, 2006). A common non-mammalian terrestrial vertebrate taxon from the late Paleocene that went extinct at the P-E Boundary was *Champsosaurus*, a reptile that bore a morphological resemblance to crocodiles (Gingerich, 2006).

However, reptiles in general did not suffer substantial extinctions, in fact at least seven species of lizards have been found to have their first occurrence in Wyoming concurrent with the PETM (Smith, 2009). These lizards appear to have emigrated from other areas in North America (Smith, 2009). However, several turtles, with Asian and American associations, have their first occurrence in North America also concurrent with the PETM (Bourque *et al*., 2008; Holroyd *et al*., 2001).

Floral response to the PETM originally appeared very minimal, with pre and post-PETM floral assemblages having similar constituents, with some immigrant taxa and changes in abundance (Wing, 1998; Wing *et al*., 2005). Pre- and post-PETM flora were largely dominated by a mixture of the angiosperms Ulmaceae, Betulaceae, and Caryaceae as well as conifers from the Cupressaceae and Taxodiaceae (Wing 1998; Wing *et al*., 2005) More recent studies have documented short lived transient floral changes in the Western Interior during the peak of the PETM dominated by members of the Fabaceae with dry tropical to subtropical associations (Smith *et al*., 2007; Wing *et al*., 2005, 2009). Globally during the PETM there is a shift to

decreased abundance of conifers and increase abundance of angiosperms based on biomarker and palynological evidence (Sluijs *et al*., 2006; Schouten *et al*., 2007).

Late Paleocene floras globally are generally low in diversity. At the P-E boundary, many of these late Paleocene plants persist, although they become less abundant (Harrington 2001; Wing *et al*., 2003, 2005, 2009).During the PETM there are also a number of new species that first appear in North America and are likely migrants from Europe and South or Central America (Harrington, 2003; Wing *et al*., 2005, 2009). Many of these migrants appear to have travelled along the coastal regions from south to north. Though the migration occurred from south to north, it doesn't appear to be indicative of rapid continental-scale northward displacement (Harrington, 2006; Wing, 2003).

There is evidence for increased insect herbivory and specialization thought to be due to increased pCO_2 and increased temperature (Currano *et al*., 2008). At higher pCO_2 levels, the C:N ratio in plants increases, resulting in a food source that is nutritionally poor in nitrogen. Therefore, nitrogen becomes limiting, so insects must consume more food to obtain the same N supply (Currano *et al*., 2008).

Though there were obvious and marked biotic changes at the PETM boundary, there were far fewer extinctions during this event than during comparable periods of globally rapid environmental change. This is one of the reasons why the PETM is of such great interest to the scientific community, especially in light of the looming effects of modern climate change.

2.3 Environmental Changes

During the PETM a number of climatic and atmospheric changes occurred. Increased pCO_2 levels are perhaps the most significant phenomenon (Cramer & Kent, 2005). Increased

pCO_2 contributed to many other secondary effects including ocean and rain water acidification and increased global average temperatures. Changes in average temperature led to a decrease in thermal gradient from the pole to equator (Huber & Sloan, 1999). This decrease in thermal gradient may also have been exacerbated by an increase in polar stratospheric clouds, caused by increased atmospheric methane (Peters, 2000). In turn this gradient change caused changes in ocean and atmospheric circulation which impacted local, regional and global weather patterns and hydrological cycles (Huber & Sloan, 1999; Schmitz & Pujalte, 2007). Changes in hydrology affected erosion and weathering rates resulting in increased outputs of sediment to the continental margins (Boucsein & Stein 2009, Pagani *et al*., 2006b).

Increased pCO_2 also resulted in decreased rainwater and surface water pH. Increased acidity in the water led to higher terrestrial weathering and erosion rates, supported by the aforementioned Sr/Ca ratios in coccolithophorid shells (Stoll & Bains, 2003; Gibbs *et al*., 2006) as well as by the general increase in near-shelf planktonic foraminiferal productivity (Crouch *et al*., 2001, 2003). Ultimately, pCO_2 levels likely returned to background levels due to the increase in productivity from higher nutrient inputs of weathered continental materials leading to excess organic carbon burial (Gibbs *et al*., 2006; Bowen & Zachos, 2010)

Global average temperatures increased rapidly due to the increase of pCO_2 during the PETM. It is estimated that maximum temperatures may have been reached within 10kyrs after the onset of the PETM (Pagani *et al*., 2006a; Aziz *et al*., 2008; Bowen *et al*., 2001; Magioncalda *et al*., 2004). Sea surface temperatures derived from foraminiferal Mg/Ca ratios and carbonate $\delta^{18}O$ show that there was an increase of 4-5º C in the tropics, 5-6º C in mid-latitudes, and upwards of 8º C in high latitudes during the PETM (Bralower *et al*., 1997, 2002; Harrington *et al*., 2003, 2006; Zachos *et al*., 2006). TEX86 biomarkers in Arctic marine sections indicate a 5-8º

C increase in average sea surface temperature (Sluijs *et al*., 2006; Weijers *et al*., 2007). Estimates based on leaf margin analysis, fish scales, mammalian teeth and soil nodules in mid-latitude terrestrial interior sections yield temperature changes of 5-7º C (Bowen *et al*., 2001, Fricke &Wing, 2004, Fricke *et al*., 1998, Koch *et al*., 2003, Wing *et al*., 2005).

Deep ocean temperature rises were commensurate with those of tropical sea surface temperatures, calculated to have increased by 4 to 5º C (Higgins, 2006). This would suggest that in the tropics there was essentially no thermal gradient driving circulation between the surface and bottom waters, which further corroborates earlier assertions about the effect of potential ocean stratification on the extinction of benthic foraminifera (Higgins, 2006; Bralower *et al*., 1997, 2002).

Warming may have been even more pronounced in high latitude polar regions. Model evidence suggests that polar interiors may have increased in temperature by as much as 10-15º C (Huber& Sloan, 1999). These greater temperatures may have been due to warmer sea surface temperatures in polar regions and the potential for increased polar stratospheric cloud formation due to increased atmospheric methane (Peters, 2000). This would be consistent with evidence which suggest high latitude migrations of APA mammalian taxa and floral taxa (Peters, 2000).

With higher average temperatures and a decrease in the pole to equator thermal gradient, there is evidence for greater moisture transport toward the poles. This change in polar precipitation was sufficient to cause a 55 ‰ shift in the D/H ratio of polar meteoric water (Pagani *et al*., 2005) and had a significant impact on local hydrology (Schmitz *et al*., 2007). Other areas showed similar changes in precipitation locally. In some cases there was an overall

annual increase and in others there was an increase in seasonal and/or large episodic precipitation events (Schmitz *et al*., 2007; Foremen & Heller, 2009)

The increase in atmospheric pCO_2 during the PETM is presumed to have resulted in higher concentrations of dissolved CO_2 in ocean water, leading to increased ocean acidity (Panchuk, 2008; Zachos *et al*., 2005). There is evidence which supports this, as marine clays and marly units during the PETM interval show depletion in carbonate concentrations relative to pre- and post-PETM intervals (Bralower, 1997; Luciani *et al*., 2007; Zachos *et al*., 2005). In some locales carbonates are completely absent at the onset of the event (Luciani *et al*., 2007). This has been interpreted as a shoaling of the carbonate compensation depth (CCD) (Bralower, 1997; Guisberti *et al*., 2007). While pH change is a plausible reason for shoaling of the CCD, several other factors may have contributed including changes in input of $CaCO_3$ from the surface ocean to bottom waters, and in remineralization rates of organic carbon and ocean circulation (Higgins & Schrag, 2006).

Chapter 3: The Hanna Basin and Its Setting

3.1 Introduction to the Hanna Basin

The western interior of North America is host to several terrestrial Paleocene-Eocene boundary sections. The Hanna Basin of south-central Wyoming contains a relatively unstudied terrestrial PETM section. In order to fully understand the PETM there, it is necessary to put it into temporal and spatial context. Here I discuss the evolution of the Hanna Basin in the context of the environmental response to this climatic event in nearby basins from the Paleocene through the Eocene.

3.2 Regional Geology

During the Paleocene and Eocene, what is now the western United States was experiencing a number of tectonic, environmental and hydrological changes. The Basin and Range Province was being created by Sevier-Laramide tectonics, causing large scale changes in altitude around the Western Interior Seaway, impacting weather patterns and changing depositional environments (Dickinson, 2003). The Western Interior Seaway began to recede, likely in part due to the aforementioned tectonic uplift, affecting local and regional hydrology, sedimentation and environmental conditions. Ecosystems and biodiversity were still recovering from the K/Pg mass extinction event through much of the Paleocene. It was during this time of tectonic and environmental upheaval in which the PETM occurred.

In the latest Cretaceous and earliest Paleocene, the Western Interior Seaway began to retreat. Contemporaneous rocks from the early Paleocene occur in several Western Interior basins including the Raton, Denver and Hanna Basin in the south and the Powder River, Williston and Big Horn Basins to the north (see figure 3.1). In these basins marine deposition

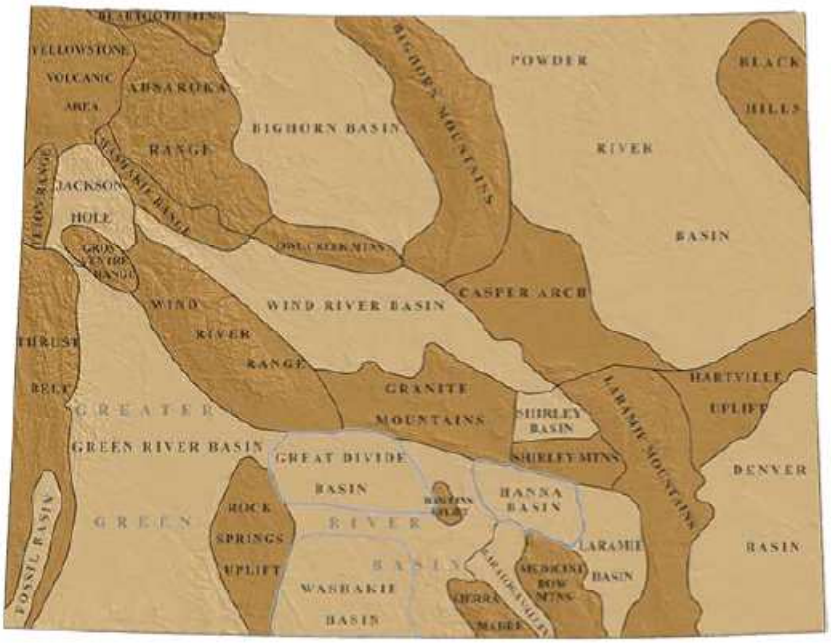

Figure 3.1 Wyoming basins map. (Wyoming State Geological Survey, 2013)

Interior Seaway occurred during the latest Cretaceous and some areas through the early Paleocene as well. These rocks, though deposited at relatively similar times, exhibit a wide range of variation in flora and fauna. This is likely due to differences in paleolatitude and location relative to the shoreline of the retreating Western Interior Seaway, but also to the advent of Laramide tectonics in the Western Interior region during this time interval (Johnson, 2002).

During the early Paleocene fossil evidence shows that the Western Interior Seaway persisted in the north in the Williston Basin. In fact there is some evidence of a re-expansion of the seaway during the early Paleocene, which has been referred to as the “Cannonball Sea” (Boyd & Lillegraven, 2011). Studies of the Fort Union Formation suggest the seaway extended

into the Bighorn Basin during the Paleocene, but had retreated locally by at least the late Paleocene (Mitchell, 2002).However, there is no evidence for the expansion of the seaway in the Paleocene into southern Wyoming (Boyd & Lillegraven, 2011). Studies of freshwater mollusk assemblages in the Paleocene age Fort Union Formation in northern Wyoming and Montana have been used to interpret paleoenvironmental conditions. The primary environments in which the molluscs lived during that time were flood basin lakes, crevasse deltas and splays. This is consistent with data showing that the Western Interior Seaway likely extended to near the vicinity of these Fort Union Formation deposits (Hanley & Flores, 1987; Mitchell, 2002).

In the Paleocene floral and faunal assemblages were still recovering from the devastation of the K/Pg mass extinction event. Coastal lowlands were slower to recover and exhibited lower diversity rates throughout the Paleocene, whereas mountainous areas with higher precipitation experienced lower extinction rates and maintained higher levels of diversity (Johnson, 2002)

The Laramide and Sevier orogenies both affected the Western Interior region greatly during the Paleocene and Eocene. As they overlapped in time and space with similar crustal shortening mechanisms, these two tectonic events are often confused (Willis, 1999). The primary difference is in the deformation type: the Laramide orogeny is characterized by uplift of basement rocks, whereas the Sevier orogeny produced more thin-skinned folding and thrusting propagating from west to east, with the eastern most folds being the youngest and exhibiting the smallest amplitudes (Willis, 1999).

The mechanisms controlling these compressional orogenic events ultimately result from the same source: subduction of the Farallon plate along the west coast of North America. The Laramide orogeny resulted in thick-skinned tectonics due to the coupled nature of the basement

and overlying sedimentary strata in the southern Western Interior; the uplift of basement rocks is thought to have occurred due to the inability of overlying sedimentary rocks to decouple from the basement rocks (Willis, 1999). There was rapid uplift of the basement rocks around 65 million years ago across the Western Interior, focused in the south (Hildebrand, 2007; Dickinson, 2003).

At the same time, further north in Montana there was a relatively simple eastward progression of thrusting events in the Sevier-associated Lewis thrust system and also in the Sawtooth Range. This resulted in a very rapid shortening in the continental crust which persisted until approximately 52 Ma, with a shortening rate of approximately 5.9 mm/yr (Fuentes *et al*., 2012). When compression ceased between the middle Eocene and early Miocene, commonly attributed to a hiatus in Farallon subduction, this tectonic regime collapsed and resulted in extension at the base of sedimentary basins within the Lewis thrust system and Sawtooth Mountains (Fuentes *et al*., 2012; Dostal *et al*., 2008). The Sevier thrust belt to the south is much better studied, but compression and shortening there did not persist into the Cenozoic.

The Basin and Range province mostly formed after these two major orogenic events. However, it is now known that the Basin and Range is a composite of multiple events in the Cenozoic, the first of which began in the Late Paleocene and continued into the Middle Miocene (Dickinson, 2003). Slab rollback of the subducting plate beneath the thickened western North American interior resulted in extension, which precipitated uplift and exposure of metamorphic basement rocks. Slab rollback also induced arc volcanism (Dickinson, 2003).

Newly uplifted ranges that resulted from these three coincident tectonic events in the Western Interior had major impacts on precipitation, drainage and the regional hydrological

cycle. During the PETM Wyoming basins in particular show abundant leaf macrofossils and a multitude of thick coal seams consistent with high rainfall and moist conditions. This is attributed to Laramide ranges creating an orographic effect whereby rain falls on the windward side with a rainshadow on the leeward side, creating very moist conditions on the windward side (Johnson, 2002).

Studies of alluvial and avulsion deposits at Polecat Bench, WY in the pre-PETM through PETM recovery interval suggest that the PETM deposits were the result of slower rates of sediment accumulation coupled with an increase in episodic deposition during the PETM with respect to pre- and post-PETM deposits (Kraus & Riggins, 2007).This pattern would be consistent with a local drying of the region during the PETM and an increase in seasonal rainfall variability (Kraus *et al*., 2008). The Willwood Formation in the Bighorn Basin contains alluvial deposits which also suggest transient drying in the region during the PETM interval (Smith *et al*., 2008). Climatic controls have been invoked as the reason behind these changes in deposition (Woody *et al*., 2007).

Other fluvial systems also experienced marked changes during the PETM. In the Clarks Fork Basin of northwestern Wyoming, sand body thicknesses increased by an order of magnitude during the PETM interval (Foreman & Heller, 2009). These changes in thickness were accompanied by a transient change in flow direction from north-northwest before the PETM to north-northwest during the PETM. The cause for these changes in fluvial systems was determined to be changes in precipitation patterns during the PETM (Foreman & Heller, 2009).

3.3 Hanna Basin Geology

Formed during the Laramide Orogeny, the Hanna Basin and its fill are the result of uplift and erosion of adjacent mountains in the Sweetwater Arch during the peak of local Laramide tectonism (Higgins, 2003; Lillegraven & Snoke, 1996; Lillegraven *et al*., 2004).

The Hanna Basin contains many formations, but the bulk of its stratigraphic thickness is comprised by the youngest rocks of the Ferris, the Medicine Bow and the Hanna Formations (see figures 3.2, 3.3). These are dominated by estuarine and fluvial channel deposits formed respectively by the retreating interior seaway and by incision events related to local sea level changes and uplift events associated with the Laramide orogeny (Lillegraven *et al*., 2004).

The Medicine Bow Formation is Maastrichtian in age and is an estuarine sequence deposited while the Western Interior Seaway still extended into southeastern Wyoming. The unit principally consists of lenticular sandstones forming channel belts interspersed with mudstones. The sandstones tend to coarsen upwards in the section, perhaps indicative of the retreating interior seaway (Landon, 2001).

The Paleocene age Ferris Formation is dated at 66-62 Ma and is characterized by sandy channel deposits and valley fill rich in coal-bearing layers. This is interpreted as the record of cyclic incision events caused by local sea level changes. Incision events created valleys which were then filled with alternating fluvial and estuarine channel deposits. These incision events are thought to have been caused by changes in local sea level at the time of deposition (Wroblewski, 2005; Boyd & Lillegraven, 2011).The Ferris Formation has thus been interpreted as continental deposits formed after the Western Interior Seaway had fully retreated from the area (Wroblewski, 2005). However, Wroblewski (2008) has argued that the Ferris Formation contains evidence for strong tidal influence on channel sediment deposition during the early Paleocene,

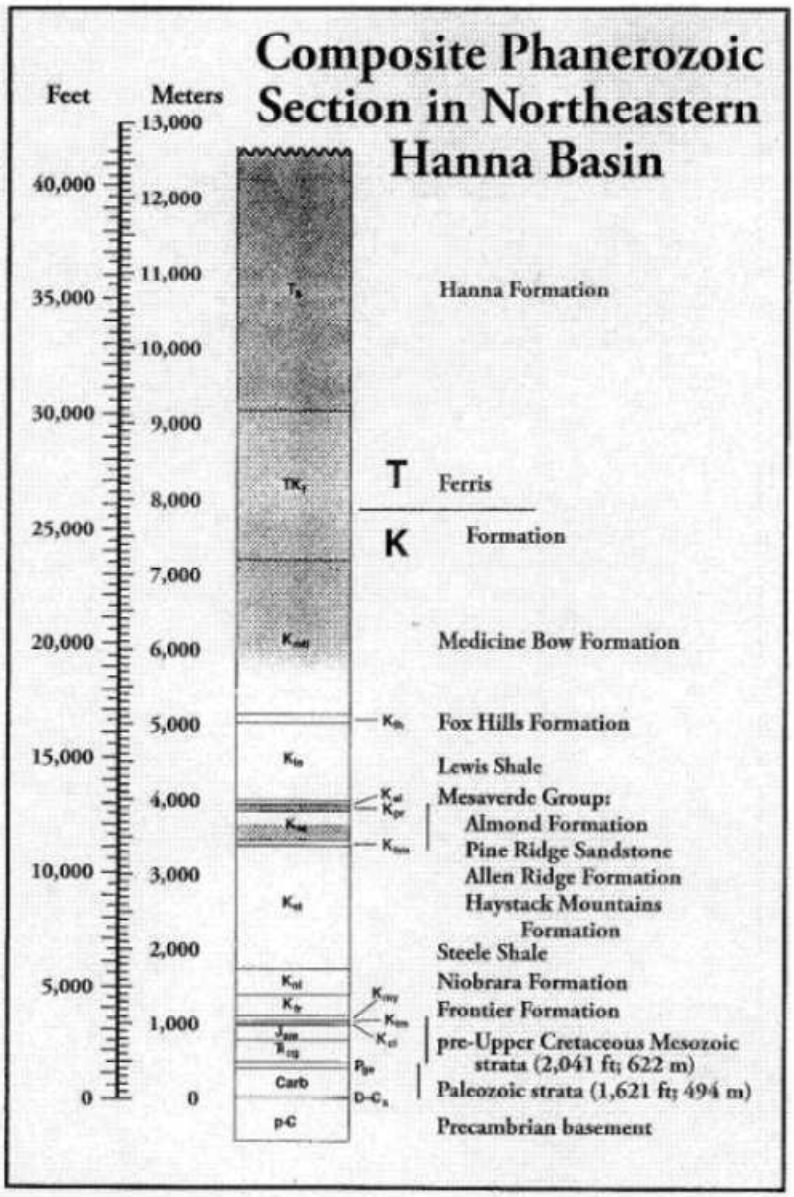

Figure 3.2 Composite section of the Hanna Basin Stratigraphy (Lillegraven *et al.*, 2004)

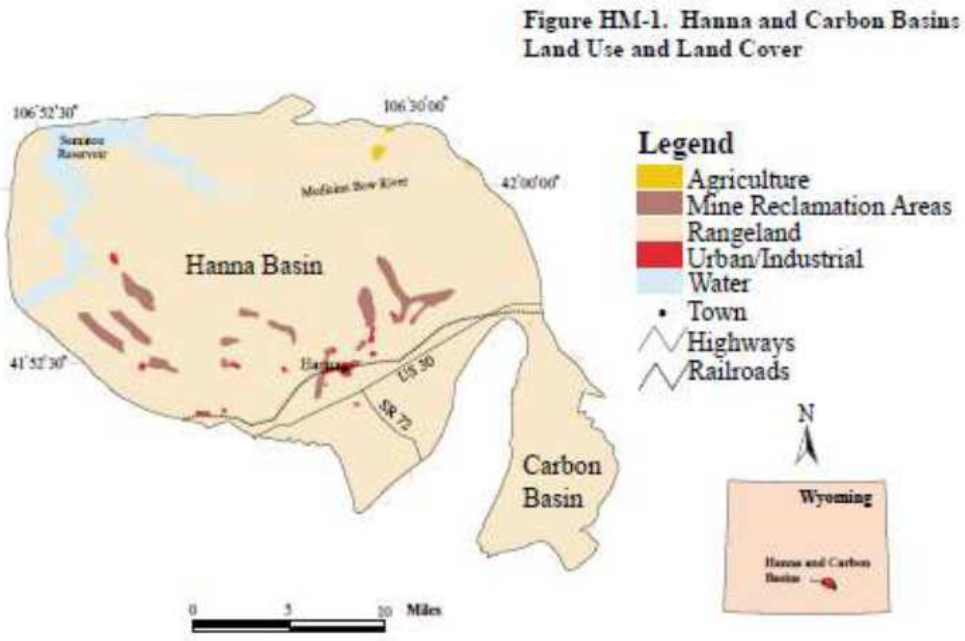

Figure 3.3 Hanna Basin, field locality marked in red. (USGS, 1999).

which suggests that the Western Interior Sea may have persisted nearer and longer in this area than previous reconstructions suggested (Wroblewski, 2008).

The Hanna Formation contains a relatively unstudied terrestrial PETM section spanning the interval from approximately 62-55 Ma and located in southern Wyoming's Hanna and Carbon Basins (Wroblewski, 2004). The Hanna Formation is comprised of sediments formed during the uplift and erosion the Sweetwater Arch during the Laramide Orogeny (Higgins, 2003; Lillegraven & Snoke, 1996; Lillegraven *et al.*, 2004).The rapidity with which uplift and subsequent erosion occurred led to high rates of sedimentation in the Hanna Formation,

estimated at upward of 0.3mm/ yr in some areas resulting in an overall thickness of greater than 3000 meters (Higgins 2000, 2003; Lillegraven *et al*., 2004).

At the field locality for this study, the Hanna Formation lies unconformably atop an erosional surface on the Steele Shale, which is a marine sequence of Upper Cretaceous age (Lillegraven & Snoke, 1996). However, due to faulting the Hanna Formation lies uncomformably above several other Upper Cretaceous formations in other locations around the Hanna Basin including marine sandstone of the Haystack Mountain Formation and nonmarine sediments of the Allen Ridge Formation. More usually, however, the Hanna Formation lies conformably above the Ferris Formation (Boyd & Lillegraven, 2011).

Spanning the late Early Paleocene through the earliest Eocene, the Hanna Formation is dominantly composed of organic-rich floodplain and fine-grained alluvial fan deposits, ideal facies for preservation of fossil plant material. As with the Ferris Formation, the Hanna Formation is largely characterized by channel fills. In the lowest section of the Hanna Formation (Torrejonian - middle Tiffanian) there are three distinct phases or zones of deposition as established by Wroblewski (2000). The first phase is dominated by fluvial sandy and gravelly channel fill deposits, interbedded with small amounts of carbonaceous shale and paleosols. This was followed by a silty to sandy phase of fluvial channel fills. In this second phase carbonaceous shales are much more abundant, many containing sideritic zones. Numerous vertebrate fossils are found in the second phase, which have been used to establish the presence of the Hanna Formation across the central and northeastern Hanna Basin and into the neighboring Carbon basin. The final depositional phase of the lower Hanna Formation is lithologically similar to the first phase (Wroblewski, 2000).

Located in the upper half of the Hanna Formation, there are two distinct units of lacustrine to marsh deposits. These units are known as the lower and upper lacustrine units (Lillegraven *et al*., 1996). Previous palynological and bulk organic carbon analysis suggest that the onset of the PETM (as marked by the CIE onset) is located in a fluvial unit situated between these two lacustrine units (Higgins, unpublished). However, the exact location of the Paleocene-Eocene (P-E) boundary has not previously been confirmed in the Hanna Basin. The thickness and organic-rich nature of these deposits makes the Hanna Basin an ideal location to investigate climate change through preserved fossil floral assemblages from across the P-E boundary (Lillegraven & Snoke, 1996).

This thesis study focuses on the lower lacustrine unit, the intermediate fluvial unit and the upper lacustrine unit, which lie a few hundred meters above the 3 lower depositional phases described by Wroblewski (2000). The intervening succession is dominated by alternating sequences of quartz-rich fine to medium grained sandstone, carbonaceous shale and lignite with very occasional cobble-sized conglomerates. Sandstones are sometimes laminar-bedded and some are in channel deposits (Lillegraven & Snoke, 1996). Within these layers siderite concretions, crayfish burrows and fish bones are commonly found (Hasiotis & Honey, 2000).

The lower lacustrine unit extends from approximately 2260-2330 meters in the local section and is mostly composed of thin laminar beds of fine to medium grained quartz-rich sandstone separated by large bodies of carbonaceous shale. The sandstones are laterally extensive and can be continuously observed for miles. The sandstones grade upwards into quartz-rich siltstone and carbonaceous shales, with some very thin coal deposits, followed by mudstone and very thinly bedded shale.

The fluvial unit, which extends roughly from 2330- 2630 meters above the base of the Hanna Formation, is also characterized by carbonaceous shales, punctuated by 2-4 meter thick layers of fine to medium grained sandstone commonly cemented with siderite and interspersed with layers of coarse siltstone. The thickest sandstone layers are found near the top of the fluvial unit, where a roughly 4 meter thick sandstone bed can be found, with submeter-scale crossbedding features. The carbonaceous shales commonly contain carbonized wood fragments and often also have sideritic pieces of petrified wood ranging in size from centimeter-scale fragments to nearly complete tree trunks with up to 20-30 centimeter diameters. These trees are often aligned as if deposited in a stream or river. Higher in the section numerous other plant fragments are preserved including carbonized leaves, leaf cuticle, and disarticulated roots and stems. Lower in the section siderite concretions are quite common. The sandstones tend to be more quartz-rich in the fluvial unit than those found in the upper lacustrine unit, indicating there may have been a change in source region between the deposition of the fluvial unit and the upper lacustrine unit.

The upper lacustrine unit lying 2630-2960 meters above the base of the Hanna Formation is dominated by cycles of carbonaceous shales grading up into carbonaceous shales containing thin beds of lignite, followed by less carbonaceous shales and occasionally laterally discontinuous freshwater limestones. These cycles are interspersed with weathering-resistant feldspathic sandstones, increasing in feldspar content up-section. This is likely due to increased erosional inputs during the uplift of the Sweetwater Arch mountains as part of local Laramide tectonics during the PETM interval. These sandstones are often interbedded with siltstones forming thin, ripple marked laminations. Fine grained carbonaceous shale layers often contain plant fossils such as carbonized wood, amber, and leaf cuticles. Sandstones often show

pronounced ripple marks, and fossil molluscs are prevalent including occasional bivalves. As with lower in the section, siderite cement is common in sandstones of the upper lacustrine unit. It should be noted, however, that based on sedimentology this lacustrine unit was likely more of a bog or marsh habitat than a true lake (Lillegraven *et al*., 2004). The top of the Hanna Formation is an erosional surface, which marks the top of the local stratigraphic sequence in the Hanna Basin (Lillegraven & Eberle, 1999). This is unsurprising given that the greatest compression and uplift in the Hanna Basin occurred during or directly after the deposition of the Hanna Formation (Lillegraven & Eberle, 1999).

Chapter 4: Palynology

Abstract

The P-E boundary, approximately 56 Mya, coincides with a global climatic event, the Paleocene-Eocene Thermal Maximum (PETM). This study aims to establish the stratigraphic location of the PETM in the Hanna Formation in the Hanna Basin, WY using palynological techniques. The first occurrence of *Platycarya platycaryoides*, an indicator species for palynozone E1, which represents the early Eocene in North America, occurs at approximately 2540 meters above the base of the Hanna Formation. This evidence suggests that the onset of the PETM isotopic excursion, which is coincident elsewhere with the Paleocene-Eocene boundary, should also be located at approximately 2540 meters above the local base of the Hanna Formation.

4.0 Introduction

The Hanna Formation spans the late Paleocene to earliest Eocene (Kirschner, 1984; Lillegraven *et al*., 2004). The largest challenge in locating the precise location of the P-E boundary and thus the PETM in the Hanna Formation is the lack of material suitable for chronometry. Therefore, chemostratigraphy and biostratigraphy are the primary means of placing temporal constraints on chronostratigraphic boundaries. Unfortunately, in large portions of the succession, there is a complete lack of vertebrate fossil preservation. Thus previous attempts to constrain the P-E boundary in the Hanna Formation have utilized fresh water mollusks and very limited palynological studies. Fresh water mollusks were examined in a study by Kirschner (1984), in which late Paleocene species were found at approximately 2350 meters above the base of the Hanna Formation. A very limited palynological study of the Hanna Formation yielded a

first occurrence of *P. platycaryoides*, an indicator species for the Early Eocene, at approximately 2800 meters above the base of the Hanna Formation (Lillegraven *et al.*, 2004).

This current study is the first to do a comprehensive palynological study of the stratigraphic interval known to span the PETM, coupled with bulk organic carbon isotopic measurements reported separately. Because previous studies had pinpointed the section of the Hanna Formation between 2300 meters and 2900 meters as the potential site of the Paleocene-Eocene boundary, and thus the PETM, this interval became the focus of this detailed palynological study.

Regional PETM Palynology

In other sections in Wyoming and around the western United States, large shifts in floral assemblages around the PETM have been observed, consisting largely of changes in abundance of pre-PETM taxa and the addition of Eocene migrants from Europe and South America (Harrington, 2003; Wing *et al*., 2003). Some of the most well studied paleofloral records in the Western Interior are located in the Powder River and Bighorn Basins in Wyoming to the north of Hanna Basin, so comparison with the taxa found in those two basins allows regional comparison of common palynomorphs found in the Hanna Basin.

Within the Powder River Basin the primary palynological studies have been focused in the vicinity of Chalk Butte (Wing *et al*., 2003). The Chalk Butte study focused on 9 samples across the PETM interval. The most common palynomorphs in those 9 samples were fern spores, taxodiaceous conifers, *Caryapollenites, Polyatriopollenites vermontensis, Ulmipollenites* and *Betulaceae/Myricaceae* (Wing *et al*., 2003). Common constituents of lower abundance at Chalk Butte included *Cycadopites scabratus, Momipites,* and *Alnipollenites* (Wing *et al*., 2003). *Cycadopites scabratus* is not present in Bighorn Basin PETM sections. In the Big Horn Basin

transient species existed during the peak of the event, followed by a new stable flora establishing itself after the PETM (Wing *et al*., 2005). *Momipites* and *Alnipollenites* respectively show approximately 5-10% and 1-8% relative abundance in the Bighorn Basin, whereas these same palynomorphs do not exceed 2% in Chalk Butte assemblages, indicating the the plants that produced these palynomorphs may have been less significant in the Chalk Butte flora (Wing & Harrington, 2001; Harrington, 1999). The difference in abundance of these palynomorphs in the Bighorn and Powder River Basins is of note, because this thesis study also noted local differences in abundance of these two palynomorphs relative to other Wyoming PETM sections.

Platycarya platycaryoides, an indicator of the early Eocene in North America, is nearly absent at Chalk Butte and is absent from the first half of a well-studied 40 meter PETM section in the Bighorn Basin (Wing *et al*., 2003). Interestingly, *Intratriporopollenites instructus*, also known as *Tilia vescipites* of Nichols and Ott (1978), first appears in the Eocene at Chalk Butte and in the Bighorn Basin, even though it first occurs elsewhere in North American during palynozone P3 in the mid-Paleocene (Nichols & Ott 1978; Wing *et al*., 2003; Harrington, 2001). The Williston Basin, North Dakota also shows *Platycarya platycaryoides* and *Intratriporopollenites instructus* as first appearing in the early Eocene (Clechenko *et al*., 2005)

4.1 Palynological Methods

Palynological samples were collected and analyzed to see what patterns of floral assemblage change occurred in the Hanna Basin during the PETM. High resolution sampling at the sub-meter scale, where suitable rock types for pollen preservation were available, was conducted over the upper 650 meters of the Hanna Formation, spanning the mid-Paleocene to earliest Eocene, guided by previous animal fossil and palynological data. Sampling concentrated

on two units (as described by Lillegraven & Snoke, 1996) within the Hanna Formation: the upper lacustrine unit and the fluvial unit, where previous studies suggested that the P-E boundary is located (Kirschner, 1984; Lillegraven & Snoke, 1996).

The field locality can be reached from the nearest settlement, which is Hanna, Wyoming. From Hanna, travel approximately 7 miles on Highway 291/ Hanna Draw Road until reaching GPS coordinates 42° 0'16.73"N 106°30'30.67"W. Turn right to enter High Allen Ranch (see figure 4.1). Follow two tracks approximately 6 miles SE to 41°58'53.16"N 106°25'57.77"W where a campsite has been established. From the campsite the field site may be reached on foot by following sandstone ridges to the North until reaching GPS coordinates 41°58'86.91"N 106°26'00.49"W, which is the base of the measured section discussed in this paper. In order to get permission to enter the High Allen Ranch please contact Burt and Kay-Lynn Palm E-mail: palm@carbonpower.net.

Figure 4.1 Relief map of field locality, access route and surrounding area in Hanna Basin, WY. (Google, 2013)

Formatted: Font: Times New Roman, 12 pt

Sampling was focused on rock types likely to contain preserved pollen grains such as coals and carbonaceous shales. There were some gaps in sample continuity where it was not possible to collect at high resolution due to erosion, burial and/or lack of suitable facies for sampling. A total of approximately 100 palynological samples were subjected to palynological maceration following methods in Funkhouser & Evitt (1959) and Doher (1980) to extract and distill pollen grains and spores. Of the samples analyzed, approximately 20 samples yielded palynomorphs of adequate number for statistical analysis of pollen abundance (>100). Another 11 samples yielded sufficient pollen for recording occurrences of pollen morphotypes, but insufficient amounts to provide useful statistical abundances.

The maceration technique consisted of crushing approximately 2 grams of carbonaceous shale per sample, such that fragments were no larger than 5 mm. Once crushed, the samples were

Figure 4.1 Relief map of field locality, access route and surrounding area in Hanna Basin, WY. (Google, 2013)

treated with 5% nitric acid to oxidize the amorphous organic material containing the pollen and spores. Next the samples were treated with 10 ml of 5-10% potassium hydroxide to remove any humic acids, which allowed the samples to disaggregate. If the sample did not respond by immediately releasing humic acid, which can be observed visually as the sample releasing black material into solution, then 10 ml of additional potassium hydroxide was added and the sample was allowed to sit for up to 5 minutes. After the humic acids had time to release the sample was flooded with distilled water to retard further chemical reaction in order to avoid over-oxidizing the sample and compromising any pollen therein. The samples were left to stand in the distilled

Formatted: Font: Times New Roman, 12 pt

water, which was decanted and replaced 1-2 times per day over the course of 3-4 days until the distilled water was clear, indicating the removal of all the released humic acids.

The samples were then treated with 10 ml of 30% hydrochloric acid to remove carbonate minerals that would subsequently form insoluble fluorides. Again the samples were flooded with distilled water and underwent the same flooding and decanting procedure as noted above for the potassium hydroxide step. Once the distilled water over the samples was clear, the sample was subjected to the hydrofluoric acid step.

Before adding hydrofluoric acid the samples were transferred to plastic centrifuge tubes and were rinsed with 10 ml of 30% hydrochloric acid, centrifuged and the hydrochloric acid was decanted. 10 ml of full strength hydrofluoric acid was added next to remove silicate minerals, thus freeing organic matter from the mineral matrix. The hydrofluoric acid was left to sit for one day, then an additional 10 ml of hydrofluoric acid was added before centrifuging and decanting the solution. In order to ensure that all hydrofluoric acid was removed from the sample, it was rinsed with 30 % hydrochloric acid three times and then rinsed with distilled water three times to prevent degradation of the sample by long term exposure to a high concentration of hydrochloric acid.

Finally, the samples were subjected to acetolysis, a process by which organic debris (such as leaf cuticle and wood fragments) is dissolved using a mixture of sulfuric acid and acetic anhydride. In order to avoid an explosive reaction between water and acetic anhydride, the samples were first rinsed in full strength acetic acid twice, then centrifuged and decanted. A mixture of 1 ml of full strength sulfuric acid to 9 ml of acetic anhydride was then added to each sample, dissolving excess organic debris. The dissolved organics were then decanted off, ideally

leaving only pollen grains and spores in the residue. Samples were rinsed with sodium pyrophosphate until the decanted liquid was clear and then rinsed with distilled water again until the decanted liquid was clear. The clean samples were stored in scintillation vials in distilled water.

Once the macerations were complete, palynological slides were made. Slides were made only from samples that were found to contain measurable amounts of fossil pollen and spores. These samples were mixed with one to two drops of each of the following: glycerin jelly and safranin dye – either safranin o or safranin y. These dyes bind to the protein on the surface of the pollen, staining the surface and making the pollen grains and their morphological characteristics more clear under the microscope. Slides were point-counted for pollen to 500 points where possible and to no less than approximately 150 points for all slide counts that were included in the diagrams in the appendices. This was done under a light microscope at 1000 times magnification.

Diagnostic palynomorphs were identified and morphological characteristics were noted and compared with previously documented palynomorphs from this time period. Since pollen is representative of the plant assemblage from which it comes, the pollen can be assumed to indicate (at least) regional changes in plant assemblages and biodiversity, both climate dependent variables. This provides a qualitative understanding of how the climate changed through time and what the effects were on ecology in that region.

Special care was taken to identify *P. platycaryoides* pollen. *P. platycaryoides* is a member of the Juglandaceae, a group which underwent an adaptive radiation during the early Paleogene. Elsewhere *P. platycaryoides* first occurs at the P-E boundary, making *P.*

platycaryoides pollen a useful and diagnostic tool for assessing the location of the P-E boundary in the Hanna Formation.

Pollen yields varied at each site, ranging from <200 to >800 per samples, with means falling around 300 grains per sample (Wing *et al*., 2003; Harrington, 2004). Pollen abundance and diversity commonly increased in the Eocene relative to the Paleocene parts of each section, indicating there was likely higher vegetative productivity during the early Eocene relative to late Paleocene (Wing *et al*., 2003). Palynological samples were primarily lignites, as the peat bogs in which the lignites originate create an ideal setting for preservation of pollen due to the low porosity of the material and the euxinic to anoxic conditions found in the bogs (Harrington *et al*., 2005; Clenchenko *et al*., 2005).

4.2 Results

During the Paleocene, the palynomorph assemblages are much less diverse than after the PETM. The pre-PETM asssemblages are principally dominated by five taxa: *Ulmipollenites, Tilia*, *Momipites*, TCT's (Taxodiaceae/Cupressaceae Type) and *Caryapollenites* (see Plate 1).

TCT's are pollen with affinity to Taxodiaceae (bald cypress family) or Cupressaceae (cypress family), but that are often very hard to distinguish from one another. These are coniferous plants, with some evergreen and some deciduous species including *Metasequoia*. *Metasequoia* is an important species as it is one of the few extant tree species from the early Cenozoic. TCT's are very abundant, comprising up to 21% of the assemblage in the pre-PETM samples, 60 meters before the first occurrence of *P. platycaryoides*. TCT abundance declines thereafter and continues to fluctuate from 0-10% throughout the rest of the section.

Caryapollenites wodehousei and *Caryapollenites veripites* are the main Carya types present (Wilson & Webster, 1946; Nichols & Ott 1978). *Caryapollenites* species are often distinguished by polar thickenings or modifications of the exine in one pole (Nichols & Ott, 1978). Heteropolarity of pore position is a distinctive feature of modern Carya pollen, and the

Plate 1

Specimens magnified to 1000 times magnification. All specimens from the Hanna Formation in the Hanna Basin, WY. Specimens photographed using a Nikon 80i compound microscope with a Nikon Coolpix 995 camera attachment.

1. *Pityosporites sp.*, #1073
2. *Pistilipollenites mcgregorii,* #1071, Palynozone P5
3. *Arecipites sp.*, #1075
4. *Tricolpites sp.*, #1073
5. *Ulmipollenites tricostatus,* #1072
6. *Caryapollenites veripites,* #1052
7. *Platycarya platycaryoides,* #1062, Palynozone E1
8. *Tilia vescipites,* #1075, Palynozone P3
9. *Alnipollenites sp.* possibly *verus,* #1077, exhibits 5 and 6-porate morphologies.

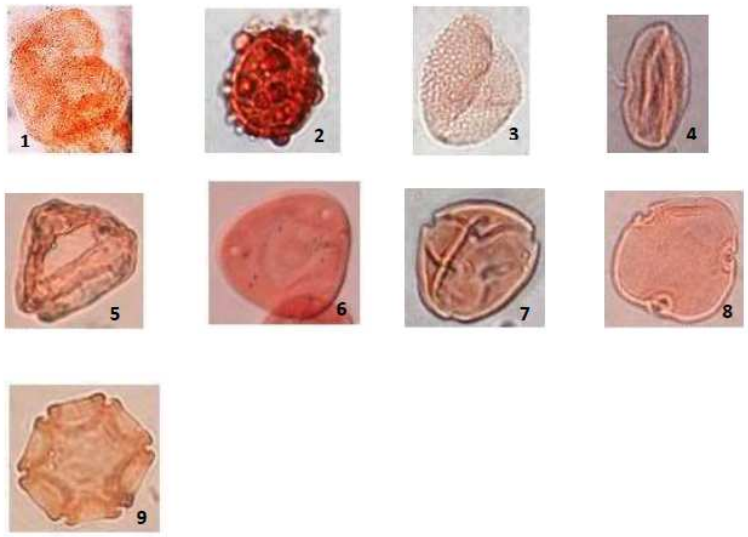

degree of heteropolarity in fossil Carya pollen serves to distinguish different fossil palynomorphs of Carya. *Caryapollenites veripites* is characterized by pores located completely in one hemisphere and a circumpolar ring of thin exine (Nichols & Ott, 1978). It differs from all other Wyoming species of the genus in this combination of features. In *Caryapollenites wodehousei* the circumpolar ring of thin exine and the pores are displaced into one hemisphere, but not completely, and the amb is notched (Nichols & Ott, 1978).

Carya types are in highest relative abundance prior to the PETM in the Hanna Basin. *Caryapollenites* morphotypes are a more ancestral member of the Juglandaceae family than *Platycarya*. *C. veripites* first occurs at approximately 2310 meters above the base of the Hanna Formation, as does *Pistilopollenites mcgregorii*. *P. mcgregorii* is a round pollen grain with a distinctive clavate surface texture, typically approximately 40 microns in diameter, and these pollen often absorb stains more readily than other pollen grains, resulting in a darker color (Pocknall, 1987). The first occurrence of these two morphotypes defines the beginning of palynozone P5, the second to last zone of the Paleocene (Nichols & Ott, 1978; see figure 4.2).

Momipites types are dominated by *Momipites wyomingensis* and *Momipites waltmanensis*. *Momipites* is also a member of the Juglandaceae family even more ancestral than *Caryapollenites*, which is thought to be derived from earlier *Momipites*-producing taxa. *Momipites* are triporate with pores arranged equatorially, more primitive and slit-like than those of *Caryapollenities* and *Platycarya* types (Nichols & Ott, 1978). Different morphotypes of *Momipites* are often differentiated by thickenings in the exine wall at the poles (Nichols & Ott, 1978). However, the two morphotypes seen in the Hanna Basin cannot be distinguished by such features. *M. wyomingensis* has no thickenings of its polar exine, nor does *M. waltmanensis* (Nichols & Ott, 1978; Pocknall, 1987).

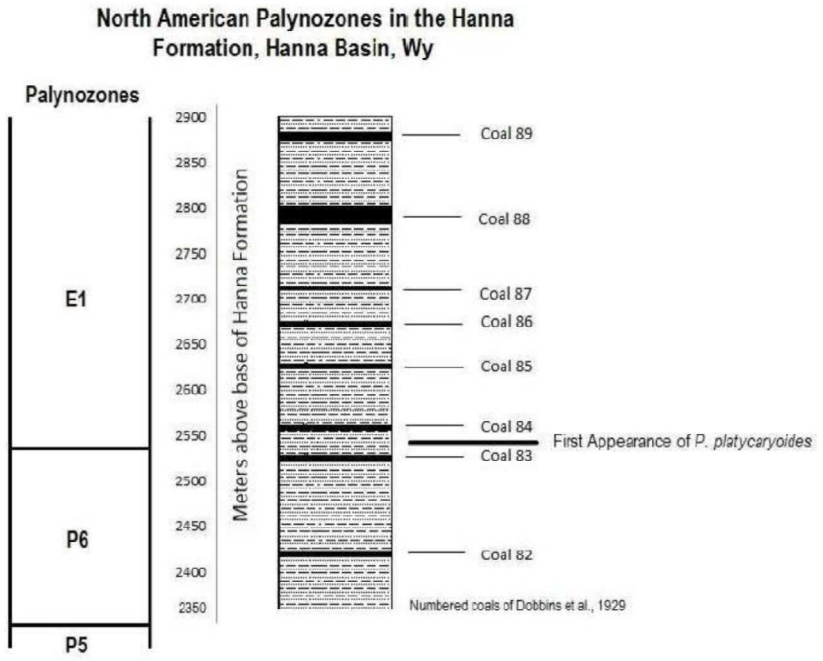

Figure 4.2 Palynozones based on pollen assemblages and abundances against stratigraphic location.

M. waltmanensis and *M. wyomingensis* both extend from palynozone P2 to P6, up until the end of the Paleocene (Nichols & Ott, 1978). *M. waltmanensis* and *M. wyomingensis* exhibit ~10% abundance below 2330 meters but taper off between 2330-2550 meters to 0% (See figure 4.3, 4.4). Between 2550-2600 meters abundance of these morphotypes increases to ~5%. Above 2600 meters abundance again tapers to 0% and both *Momipites* types disappear from the record (Nichols & Ott, 1978; Wing *at al*., 2003). *Ulmipollenites* types are dominated by *Ulmipollenites tricostatus* and *Ulmipollenites krempii. Ulmipollenites tricostatus* and *Ulmipollenites krempii* both share the distinctive regulate

Meters Above Base of Hanna Formation	*Pityosporites*	*TCT*	*Alnipollenites*	*Caryapollenites*	*Momipites*	*Pistillipollenites*	*Platycaryapollenites*	*Rousea*	*Sphaeralcea*	*Tiliapollenites*	*Tricolpites*	*Ulmipollenites*	*Insulapollenites*	*Arecipites*	Fungal Spores	Total
2301.5	1	34	0	12	12	0	0	4	0	0	8	60	0	0	80	211
2309	1	40	0	75	25	3	0	0	0	7	50	23	0	0	48	272
2316.5	0	40	0	50	10	0	0	0	0	20	39	0	0	0	30	189
2328.5	0	3	0	40	8	0	0	0	0	85	30	5	0	0	30	201
2350	0	5	0	0	0	0	0	0	0	0	4	0	0	0	10	19
2438	0	0	0	4	0	0	0	0	0	0	0	2	0	0	5	11
2475.5	0	6	5	4	0	1	0	0	0	1	2	3	0	0	10	32
2496.5	0	0	45	4	0	8	0	0	0	5	0	0	0	50	0	112
2517.5	0	11	2	0	0	0	0	0	0	0	3	3	0	0	5	24
2540	0	4	50	2	2	0	40	0	0	0	7	6	1	77	15	204
2547.5	0	5	8	0	0	2	4	0	0	0	2	0	0	3	8	32
2555	1	70	61	2	5	18	46	0	0	3	22	0	0	8	12	248
2577.5	2	46	52	4	6	4	102	0	0	0	10	0	0	8	0	234
2579	2	20	168	3	0	64	54	0	0	0	2	0	0	22	18	353
2580.5	0	26	52	10	0	3	121	0	0	2	15	18	0	15	8	270
2582	1	14	53	12	0	32	102	0	0	0	121	31	0	13	32	411
2583	1	11	36	4	11	5	112	0	0	2	0	15	0	3	0	200
2583.5	1	66	70	12	0	20	47	3	0	9	12	16	0	41	62	359
2588	2	92	11	4	0	0	5	0	1	2	2	0	0	1	22	142
2589.5	3	3	70	0	3	17	9	0	0	2	14	12	0	111	7	251
2627	3	0	140	0	0	52	45	0	0	0	61	10	50	0	20	381
2628.5	0	0	5	0	0	0	2	0	0	1	1	0	0	0	0	9
2634.5	0	6	0	0	0	0	2	0	0	0	5	0	0	0	0	13
2636	0	27	2	0	0	0	8	0	0	0	4	3	0	4	4	52
2693	1	14	25	10	0	7	13	0	0	2	11	20	0	35	65	203
2697.5	2	0	30	6	0	5	200	0	0	0	0	5	0	0	10	258
2712.5	0	2	3	0	0	0	3	0	0	1	1	2	0	1	6	19
2720	0	0	2	0	0	0	0	0	0	0	0	0	0	0	2	4
2795	0	49	42	0	0	0	10	0	0	48	31	0	0	10	75	265
2943.5		5	4	0	0	2	6	0	0	0	3	0	0	8	15	43
2946.5	1	15	5	10	0	0	8	0	0	2	2	2	0	12	145	202

Absolute Abundance of Dominant Palynomorphs in a PETM section of the Hanna Formation, Hanna Basin, WY

Figure 4.3 Absolute abundance of palynomorphs relative to stratigraphic location.

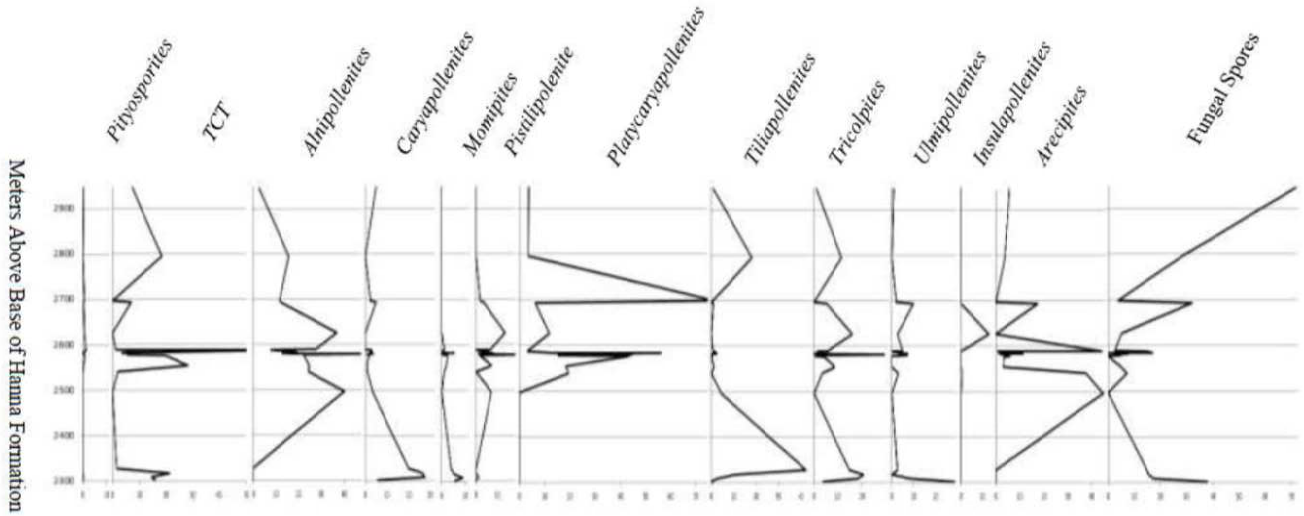

Relative Abundance of Dominant Palynomorphs in a PETM section of the Hanna Formation, Hanna Basin, WY

Figure 4.4 Relative abundance (by percentage) of dominant palynomorphs relative to stratigraphic location.

texture shared by modern Ulmus species, and they are also triporate (Pocknall, 1987). *U. tricostatus* is more triangular in shape, with thickenings extending between the pores, while *U. krempii* is more rounded, but slightly triangular and lacks thickenings between the pores. Both have roughly equatorial pore distributions (Pocknall, 1987). These *Ulmipollenites* morphotypes comprise over 25% of the pollen assemblage at the base of the measured section about 2300 meters above the local base of the Hanna Formation. The presence and relative abundance of *Ulmipollenites, M. wyomingensis* and *C. wodehousei* at this point is consistent with the *Aquilapollenites pinulosus* Zone of Pocknall (1987), which is contemporaneous with Zone P4 of Nichols and Ott (1978). The relative abundance of *Ulmipollenites* decreases drastically in the earliest Eocene in the Hanna Basin.

Tilia vescipites Nichols and Ott, 1978, also incorrectly known as *Intratriporopollenites*, is triporate with equatorial pore distribution and characteristic "C-shaped" thickenings around each pore. These pollen are typically larger than 50 microns in diameter (Pocknall *et al*., 1987). *T. vescipites* first appears in North America in zone P3. In the Hanna Basin it first appears around 2310 meters above the base of the Hanna Formation, indicating that that location is zone P3 or later (Robertson, 1975). *T. vescipites* is abundant, comprising 2-42% of the assemblage through 2330 meters above the base of the Hanna Formation. After that its abundance remains less than 3% until the recovery interval after the PETM, increasing in abundance to >10% at approximately 2800 meters, before decreasing to <1% at 2900 meters.

There is also a greater relative abundance of fungal spores, comprising approximately 15-35% of total abundance in the late Paleocene samples between 2300- 2330 meters above the base of the Hanna Formation, although they occur up to approximately 2475 meters. Fungal spores

vary in size and shape, lack pores and typically have a thicker sporopollenin exine which more readily absorbs stain, giving them a deeper color than pollen grains.

Pitysporites is a bisaccate (two-bladdered) conifer pollen and occurs in very low abundance (<1%) throughout the section. This pollen are associated most often with more mountainous regions and due to its saccate nature is very buoyant, allowing it to travel far from its source. Therefore, this pollen is often not deposited in situ and may not reflect the local ecology, but rather more of the average regional ecology of the area. The low abundance and lack of variability make this pollen of little diagnostic use to this study.

Tricolpites pollen also occurs throughout the Paleocene and Eocene, however this is a catch-all name that can encompass a number of different pollen types, which all share the same tricolpate (three-furrowed) morphology. Therefore this pollen grain is not particularly taxonomically useful.

Palynomorphs in the Hanna Basin show a gradual transition from those typical of the late Paleocene flora to the early Eocene flora. The first major change is the first occurrence of the late Paleocene palynomorph *Alnipollenites* in the section at 2475 meters. *Alnipollenites* are multiporate pollen which can vary in pore number, but are most commonly 4, 5 or 6-pored and have arci linking the pores, giving them a star or snowflake like appearance (Pocknall, 1987; Wing *et al*., 2003). In the Hanna Basin *Alnipollenites* immediately becomes a dominant floral taxon constituting 20-48% of the palynoflora in the latest Paleocene (zone P6) through the early Eocene. The rapid introduction and increase in abundance of *Alnipollenites* occurs in the fluvial unit. The increase in *Alnipollenites* is concurrent with a decreased abundance of TCT's (coniferous pollen).

Alnipollenites precedes introductions of other migratory taxa locally. *Arecipites, Platycarya, Pistilipollenites* and TCT abundances show an inverse relationship to abundances of *Alnipollenites.* In fact there appears to be a repeating pattern of *Alnipollenites* abundance fluctuating cyclically between 20-48%, and when the *Alnipollenites* abundance is near the lower bounds of that abundance range, the aforementioned four palynomorphs. The first occurrence locally of *Arecipites* directly follows the first occurrence of *Alnipollenites*. *Arecipites* is distinguished by its regulate texture and a characteristic furrow that extends from pole to pole, giving the grains an appearance similar to a coffee bean.

At 2540 meters above the base of the Hanna Formation *P. platycaryoides* first appears and is present in all subsequent samples. *P. platycaryoides* is triporate, with equatorial pore distribution and polar modification that looks like a Celtic trinity symbol (Nichols & Ott, 1978). Its occurrence is significant because the Juglandaceae family, of which *P. platycaryoides* is a member, underwent an adaptive radiation during the earliest Eocene. *P. platycaryoides* first appears in the geologic record in the earliest Eocene and is an indicator species for the beginning of North American palynozone Zone E1 (Nichols & Ott, 1978). Prior to the first occurrence of *P. platycaryoides* the dominant genera were *Ulmipollenites, Tiliapollenites, Momipites,* and *Caryapollenites*. Afterwards, in the earliest Eocene, all of these Paleocene groups decrease in relative abundance. *Caryapollenites* and *Momipites* decrease to less than 5% of the total pollen abundance and never recover their earlier abundance. *Momipites* varieties eventually disappear completely from the record.

Pistillipollenites mcgregorii and TCT (Taxodiaceae/Cupressaceae type) pollen, which were in low abundance in the late Paleocene, become more dominant in the earliest Eocene, just 15 meters stratigraphically above the first occurrence of *P. platycaryoides*. The relative

abundance of these palynomorphs changes through the earliest Eocene portion of the section with TCT's exhibiting 20-30% relative abundance between 2550-2600 meters, while *P. platycaryoides* shows an increase from 2540-2600 meters as well, comprising 30-60% of the pollen assemblage. Between 2600-2700 meters its abundance drops below 20%, but it becomes much more abundant above 2700 meters, comprising up to 70% of the assemblage. Above 2800 meters *P. platycaryoides* abundance decreases to less than 10%.

Arecipites also shows a trend of increasing abundance upwards from 0% relative abundance at 2300 meters to over 40% at 2500 meters. Then between 2500-2700 meters abundance fluctuates between <10% and 40%. Above 2700 meters *Arecipites* maintains <10% abundance. There is a trend of increasing size upwards, ranging from 20 μm lower in the section to over 40 μm higher in the section. *Alnipollenites* also shows a similar magnitude of change in grain size through the section, but also experiences a shift in relative abundance of 5 and 6-pored varieties. Lower in the section6-pored *Alnipollenites* are more prevalent, being of roughly equal abundance to the 5-pored forms. However, higher in the section 5-pored *Alnipollenites* overwhelmingly dominates the Alnus palynomorphs.

The early Eocene palynoflora in the Hanna Basin differs from the late Paleocene in that there are several immigrant palynomorphs as discussed above, but also the persisting late Paleocene flora tend to decrease in relative abundance in the Eocene, with *Momipites* eventually disappearing from the record altogether. *Ulmipollenites* in the Hanna Basin fluctuates in relative abundance during the Eocene. At 2300 meters *Ulmipollenites* comprise over 20% of relative abundance, then decrease to <5%. At approximately 2600 meters abundance increases slightly fluctuating 5-10%. Above 2700 meters abundance is <1%.

4.3Discussion

Biostratigraphy

Below 2310 meters above the base of the Hanna Formation, *Caryapollenites wodehousei* is the only *Carya* morphotype present. Elsewhere in North America *C. wodehousei* is found in zone P4 through P6 (Nichols & Ott, 1978). *C. veripites* first occurs at approximately 2310 meters above the base of the Hanna Formation, as does *Pistilopollenites mcgregorii*. *P. mcgregorii* comes from a now extinct species of plant, is characterized by clavate surface texture and a very stain absorbent exine resulting in a deeper color than many other palynomorphs. The presence of *P. mcgregorii* is significant, because the first occurrence *P. mcgregorii* and *C. veripites* is what defines the beginning of palynozone P5, the second to last zone of the Paleocene (Nichols & Ott, 1978).

Therefore, the presence of *C. wodehousei* and the absence of *C. veripites* imply that below 2310 meters the rocks may be P4 in age (Nichols & Ott, 1978), but there are insufficient numbers of samples at that level in the section to make a positive assignment. Furthermore, the presence and relative abundance of *Ulmipollenites, M. wyomingensis* and *C. wodehousei* below 2310 meters is consistent with the *Aquilapollenites pinulosus* Zone of Pocknall (1987), which is contemporaneous with Zone P4 of Nichols and Ott (1978). However, as this assignment is based on abundances in only one palynological sample, this conclusion must remain tentative.

The lower abundance of these two *Momipites* types above 2330 meters and the higher abundance of *C. veripites* are consistent with this point marking the transition from zone P5 to P6 where the relative abundance of these two groups of pollen switch (Robertson, 1975). This is not a conclusive placement of the boundary between P5 and P6 as P6 indicator species are absent, but it is the best inference of the placement of the P5-P6 boundary that can be made with

the available data. *Platycarya platycaryoides* is the primary indicator species in North America for the P6-E1 boundary, concurrent with the P-E Boundary (Nichols & Ott, 1978).

Comparisons with nearby P-E sections

Overall, the Hanna Basin palynoflora shows lower species diversity than adjacent contemporary basins. But due to the limited number of palynological samples which yielded high pollen counts (>200 grains), it is possible that this lower diversity in the Hanna Basin may be a sampling artifact. Future work should seek to increase sample size and/or use rarefaction to accurately compare measures of species diversity.

U. krempii in the Wind River and Powder River Basins maintains a high relative abundance into the earliest Eocene (Wing *et al*., 2003; Pocknall, 1987). However, in the Hanna Basin the relative abundance of this species decreases drastically in the earliest Eocene, evidence for some local variability in dominant palynomorphs in the Hanna Basin relative to other Wyoming P-E sections.

In the Hanna Basin *T. vescipites* is very abundant in the late Paleocene, but becomes less abundant in the earliest Eocene. In the nearby Wind River, Powder River and Bighorn Basins that are further north, however, *T. vescipites* first occurs in the early Eocene, despite the fact that it first occurs in North America in zone P3. It maintains high abundances and is useful as an indicator of the earliest Eocene in those basins (Pocknall, 1987; Wing *et al*., 2003). The Williston Basin in North Dakota shows a similar early Eocene first occurrence for *T. vescipites* (Clenchenko *et al*., 2005). This may be indicative of paleoenvironmental conditions that were not conducive to *T. vescipites* or could be further evidence to argue for a northward migration of some flora species during the PETM (Harrington, 2003; Wing *et al*., 2003). As with the

Ulmipollenites morphotypes, this is a difference in relative abundance trends for pollen in the Hanna Basin relative to other Wyoming P-E boundary sections.

Alnipollenites occurs in low abundance (>2%) in the Powder River Basin from the late Paleocene to early Eocene and also occurs in the Bighorn Basin during that time, with a 4-6% increase in abundance in the early Eocene. In the Hanna Basin *Alnipollenites* also has its first occurrence in the late Paleocene, but immediately becomes a dominant floral taxon constituting 20-48% of the palynoflora in the latest Paleocene (zone P6) through the early Eocene. The rapid introduction and increase in abundance of *Alnipollenites* occurs in the fluvial unit, which has been associated with changes in local tectonic uplift, possible change in precipitation and or sea level (Lillegraven *et al*., 2004).

Arecipites is in the palm family and has paratropical associations, being common in Gulf Coast PETM sections from Mississippi and Alabama (Harrington *et al*., 2004). In northern Wyoming, this palynomorph is present in the Paleocene of the Powder River Basin but has very low abundance in the Eocene, and is absent from the Bighorn Basin (Wing *et al*., 2003; Harrington, 1999; Wing and Harrington, 2001).

The Paleocene flora in the Hanna Formation shows a high relative abundance of *Tilia vescipites*, which doesn't occur in the Bighorn and Powder River Basins until the Eocene (Wing et al., 2003). Additionally, *P. platycaryoides* is prominent in the earliest Eocene in the Hanna Basin, while it is nearly or completely absent from early Eocene sections in the Bighorn and Powder River Basins (Wing & Harrington 2001; Harrington 1999). Finally, *Alnipollenites* shows a near order of magnitude higher relative abundance in the Hanna Formation than in the Bighorn or Powder River Basins (Wing & Harrington 2001; Harrington 2001b).

There is also a greater relative abundance of fungal spores in the Hanna Formation, comprising approximately 15-35% of total abundance in the late Paleocene samples between 2300-2330 meters. The higher fungal spore counts occur where the late Paleocene flora also occur. This may indicate a temporary increase in decaying organic material, which could have resulted from changes in regional climate and weather patterns or from changes in depositonal setting.

At 2540 meters above the base of the Hanna Formation *Platycarya platycaryoides* first appears and is present in all subsequent samples. This pattern differs from that of other Wyoming basins, which are nearly devoid of *P. platycaryoides* altogether or the morphotype does not occur until well into the early Eocene (Wing *et al*., 2003)

Alnipollenites abundance is much higher in the Eocene in the Hanna Basin where its abundance exceeds by nearly an order of magnitude the relative abundance increase of *Alnipollenites* in the Bighorn and Powder River Basins (Wing & Harrington 2001; Harrington 2001b). Additionally, the Hanna Basin sees a decrease in relative abundance of *Ulmipollenites* in the Eocene, while the opposite is true in the Bighorn and Powder River Basins (Wing *et al*., 2003).

The later occurrence of *T. vescipites* and *P. platycaryoides* elsewhere may indicate a northward migration of these species or slight regional environmental differences which made the Hanna Basin more hospitable to these floral types. The decrease in *Ulmipollenites* during the early Eocene may have provided an opportunity for Alders to grow in abundance due to decreased light competition.

The Hanna Formation largely agrees with previous studies in nearby basins as to the paleofloral evolution in the Western Interior during the PETM. It does show some local and regional differences due to closer proximity to the Gulf Coast and differing uplift history. Palynological evidence supports the stratigraphic location of the PETM as being between 2600-2650 meters above the local base of the Hanna Formation. Six-pored *Alnipollenites* are more prevalent, being of roughly equal abundance to the 5-pored palynomorph. However, higher in the section 5-pored *Alnipollenites* overwhelmingly dominates the Alnus palynomorphs.

Environmental Causes of Palynological Changes

There is a transient fluvial layer in which *Alnipollenites* first occurs and that layer may represent either a change in uplift and associated erosion and deposition rates or a change in precipitation, as seen in other PETM sections (Smith *et al*., 2008; Kraus *et al*., 2007; Lillegraven & Snoke, 1996; Higgins, 2000, 2003). In any of those scenarios it is likely that there was a disturbance of the soil with increased weathering and erosion rates concurrent with observed changes in floral abundance and occurrence. The decrease in coniferous trees and Elms would corroborate this and provide an opening for Alders, with decreased competition from coniferous canopy trees. Additionally, Alders are often pioneer species in disturbed habitats due to the symbiotic relationship with Nitrogen-fixing bacteria in Alder root nodules (Virtanaen *et al*., 1954). Therefore, it is plausible that the introduction and proliferation of *Alnipollenites* was due to increased local disturbance creating a habitat that was inhospitable to other floral taxa, providing an opening for Alders. However, it is not clear whether the continually high alder concentration implies stable, “climax” alder populations or continous sediment disturbance, promoting dominance of disturbance-loving alders.

The increase in *Alnipollenites* is concurrent with a decreased abundance of TCT's, which may be due to changes in canopy structure. Fewer large canopy trees, like Taxodiaceae and Cupressaceae are present, allowing for the expansion of understory species such as *Alnipollenites*. Additionally, the shift in deposition type from a bog or lacustrine environment in the lower lacustrine unit to the fluvial deposition in the fluvial unit may have resulted in taphonomic bias. Lakes tend to preserve more regionally averaged palynofloras as they act as a catchment for regional fluvial sources, which carry pollen. Additionally, lakes receive wind-transported pollen from distant areas. Conversely, fluvial systems tend to deposit and record more local vegetation that grow directly around the fluvial or riverine system.

Alnipollenites appearance precedes introductions of other migratory taxa locally. Increases in *Arecipites*, *P. platycaryoides*, *Pistilipollenites* and TCT's follow the increase in *Alnipollenites*. In fact there appears to be a pattern of increase abundance of *Alnipollenites* followed by concurrent decreases in *Alnipollenites* while other dominant flora increased in abundance. This would be consistent with repeated local disturbance events, which is concordant with regional changes in uplift and erosion rates and evidence from other PETM localities for altered precipitation and sedimentation during the PETM (Foremen & Heller, 2009; Lillegraven & Snoke, 1996).

Porosity of multi-porate pollen grains has been suggested to correlate with moisture and temperature conditions. The noticeable change in alder pollen porosity should be investigated in future studies to see if this change may be correlated to environmental change.

The primary discussion of palynological evidence in this paper has focused on relative abundance of palynomorphs. There is some evidence to suggest that a number of factors including productivity, temperature and depositional setting can affect the relative abundances of pollen and may not directly reflect changes in floral composition (McInerney & Wing, 2011).

Therefore it is also will be important in future work to consider absolute abundances of pollen throughout the PETM section in the Hanna Basin in the context of these additional factors.

4.4 Conclusion

The measured section in this study spans the palynozones P5 and possibly P4 through E1, representing the late mid-Paleocene to the earliest Eocene. Palynological data suggest a major shift in the floral composition and abundances between the Paleocene palynozones and the Eocene palynozone. The Eocene shows a more diversified floral assemblage, although rarefaction analysis is needed to properly evaluate differences in diversity. The Hanna Basin Paleocene flora is similar to those found in Powder River and Bighorn Basins in that all three show a higher abundance of *Momipites* and *Caryapollenites* than other Western Interior locations (Wing & Harrington 2001; Harrington 2001b). However, there are some key differences. The Hanna Formation shows a high Paleocene abundance of *Tilia vescipites*, which doesn't occur in the Bighorn and Powder River Basins until the Eocene (Wing *et al*., 2003). Additionally, the relative abundance of *Ulmipollenites* in the Hanna Basin is higher in the Paleocene than in the Eocene while both the Powder River and Bighorn Basins show the opposite pattern of *Ulmipollenites* relative abundance through time (Wing & Harrington 2001; Harrington 2001b).

The later occurrence of *T. vescipites* and *P. platycaryoides* may indicate a northward migration of floral species or slight regional differences in environment, which made the Hanna Basin more hospitable to these floral types. The decrease in *Ulmipollenites* during the early Eocene along with increases in Alder may be indicative of changes in canopy structure during the PETM.

The Hanna Formation in the Hanna Basin, WY largely agrees with previous studies in nearby basins as to the paleofloral evolution in the Western Interior during the PETM. It does show some local and regional differences due to closer proximity to the Gulf Coast and differences in uplift history. Palynological and isotopic evidence support the stratigraphic location of the PETM interval as being between approximately 2550-2650 meters above the local base of the Hanna Formation. This constitutes a considerable increase in the precise stratigraphic location of the PETM interval within the Hanna Basin, which was previously constrained to between 2350-2800 meters.

Additional studies are needed to further refine timing of the PETM and ecological response to the event in the Hanna Basin. Some potential additional work that should be done include phytolith studies. Phytoliths are typically siliceous deposits in intra and extracellular plant structures, thus often creating a cast of the structure (e.g., Piperno 2006). Phytoliths remain after organic material has decayed and are often preserved in paleosols and other terrestrial sediment deposits (Strömberg 2002). The size, shape and associations of these phytoliths can be used to identify what type of plant they came from and what plant structure the phytolith represents. Phytoliths, which represent leaf epidermal cells will preserve the shape of those cells. Cell shape – specifically undulation on the margin of the cells – has been correlated with light conditions, which can be used to infer changes in canopy structure (Kürschner 1997).

In addition, rarefaction studies should be conducted in order to determine if the lower diversity is an actual pattern observed in the Hanna Basin or merely a sampling artifact. Unfortunately, that work is beyond the scope of this current thesis project. However, the work done here to more precisely constrain the CIE and thus the PETM within the Hanna Formation

will allow for future studies to make more detailed studies of the paleocological and paleoenvironmental changes during this interval.

Chapter 5: Isotopic Geochemistry

Abstract

The P-E boundary, approximately 56 Mya, coincides with a global climatic event, the Paleocene-Eocene Thermal Maximum (PETM). The PETM is believed to have resulted from a 2-8 fold increase in atmospheric pCO_2 in less than 10,000 years which led to a marked carbon isotope excursion (CIE). The increase in pCO_2 and the resulting global warming was accompanied by numerous paleoecological and paleoenvironmental changes. This study aims to establish the stratigraphic location of the PETM in the Hanna Formation in the Hanna Basin, WY. Bulk organic carbon isotope measurements of organic rich carbonaceous shales and lignites were performed with a continuous flow isotope-ratio mass spectrometer. A negative carbon isotope excursion of approximately -2 ‰ occurred between 2600-2650 meters above the base of the Hanna Formation. Directly below the negative carbon isotope excursion is a positive isotope excursion of similar magnitude. The negative CIE is approximately 50 meters stratigraphically above the first occurrence of *Platycaryapollenites platycaryoides*, an indicator species for palynozone E1, which represents the early Eocene in North America. This evidence suggests that the CIE, which characterizes the onset of the PETM, did not commence at the Paleocene-Eocene boundary but instead was somewhat delayed in the Hanna Basin

5.0 Introduction

Previous studies have shown the Hanna Formation to span the late Paleocene to earliest Eocene (Kirschner, 1984; Lillegraven *et al*., 2004). However, the Paleocene-Eocene boundary and the concurrent onset of the PETM have not yet been precisely located stratigraphically in the section. The largest challenge in locating the precise location of the P-E boundary and thus the

PETM in the Hanna Basin is the lack of material suitable for chronometry. Therefore, chemostratigraphy and biostratigraphy are the primary means of placing temporal constraints on these stratigraphic events. Unfortunately, in large portions of the record, there is a complete lack of vertebrate fossil preservation, the main biostratigraphic tool used other nearby P-E basins. As a result, the previous attempts to constrain the P-E boundary in the Hanna Basin have utilized fresh water mollusks and very limited palynological data (Kirschner, 1984; Lillegraven *et al*., 2004). Fresh water mollusks were used in a study by Kirschner (1984), in which late Paleocene species were found at approximately 2350 meters above the base of the Hanna Formation. A very limited palynological study of the Hanna Formation yielded a first occurrence of *Platycarya platycaryoides*, an indicator fossil for the earliest Eocene, at approximately 2800 meters above the base of the Hanna Formation (Lillegraven *et al*., 2004). This is why that section of the Hanna Formation – between 2300 meters and 2900 meters - became the focus of this more detailed carbon isotope study.

In this study terrestrial bulk organic carbon samples were taken from lignites and carbonaceous shales in order to determine the carbon isotope composition of the atmosphere at the time of deposition. Bulk organic carbon is primarily composed of preserved fossil plant material. Since the plants exchanged CO_2 with the atmosphere while they were alive and there is a known fractionation between ambient CO_2 and the carbon content of photosynthetic organisms, the bulk organic carbon isotope composition can be used to reconstruct the paleoatmospheric composition during the PETM. The amount of fractionation depends on the type of plant that is photosynthesizing. There are three major metabolic pathways for photosynthesis: C3, C4 and CAM or crassulacean acid metabolism (O'Leary, 1981), with the latter two pathways yielding much heavier carbon than C3 metabolism. C3 plants represent the oldest known type of

photosynthesis with isotopic markers dating them as far back as the Paleozoic. C4 plants evidently did not originate until the Oligocene, roughly 30 million years ago (Gowik *et al*, 2011). CAM plants also originated after the PETM and only occur in very arid locations. Therefore, it is reasonable to assume that all plants alive 56 million years ago during the PETM would have utilized a C3 metabolism (Keeley & Rundel, 2003).

Although the three common photosynthetic pathways (C3, C4 and CAM) all show diagnostically different fractionations of ^{13}C during photosynthesis, there is very little variation in bulk organic isotope composition between different species utilizing the same metabolic pathway (O'Leary, 1981). The known fractionation can then be used to constrain the source of carbon-containing greenhouse gases (e.g. CO_2, CH_4) responsible for the global warming event. However, the magnitude of the CIE is directly proportional to the magnitude of atmospheric change as the photosynthesis fractionation is roughly constant regardless of atmospheric composition for C3 plants (O'Leary, 1981).

Field locality can be reached from the nearest settlement, which is Hanna Wyoming. From Hanna, travel approximately 7 miles on Highway 291/ Hanna Draw Road until reaching GPS coordinates 42° 0'16.73"N 106°30'30.67"W. Turn right to enter High Allen Ranch see (figure 4.1). Follow two tracks approximately 6 miles SE to 41°58'53.16"N 106°25'57.77"W where a campsite has been established. From the campsite the field site may be reached on foot by following sandstone ridges to the North until reaching GPS coordinates 41°58'86.91"N 106°26'00.49"W, which is the base of the measured section discussed in this paper. In order to get permission to enter the High Allen Ranch please contact Burt and Kay-Lynn Palm E-mail: palm@carbonpower.net.

In summary, bulk organic carbon isotopes provide information as to potential sources and amounts of CO2 released during the PETM. The characteristic CIE at the onset of the event can also be used as a stratigraphic constraint for the onset of the PETM in a given geologic section.

5.1 Methods

High resolution sampling at the sub-meter scale (where possible) was conducted over the upper 650 meters of the Hanna Formation spanning the late mid-Paleocene to earliest Eocene, the age of which was constrained by previous animal fossil studies and palynological data. There were some gaps in the section where it was not possible to sample at this resolution due to erosion and younger cover. Over 200 samples were collected over the course of four field seasons, mostly of coals and carbonaceous shales. The samples were crushed and homogenized, then treated with 30% hydrochloric acid to remove any pedogenic carbonates that might contaminate the organic carbon isotope signature. Samples were then rinsed three times with distilled water and dried completely. After samples were dry they were weighed into tin boats and analyzed for organic carbon isotopic content, using a continuous flow isotope-ratio mass spectrometer (Thermo Finnegan MAT 253) coupled to an elemental analyzer (Costech ECS 4010 EA).

Duplicate samples were analyzed for each sample and compared with three carbon standards: Peach Leaves (NIST 1547), glutamic acid 1 (GA1) and glutamic acid (GA2).The precision for these standards for the mass spectrometer used in this study are as follows: GA1 standard deviation of 0.12‰ (n=1797), GA2 standard deviation of 0.08‰ (n=1905), and Peach Leaves 0.1‰ (n=824). Once measurements were completed, the raw data was standardized to VPDB. Any samples for which duplicates had a higher standard deviation than that of the

standards were rerun. If the triplicates still had a higher standard deviation than the standards, the sample was excluded on the basis that the sample was either not homogeneous enough to yield accurate results or there was a significant error in the analytical process which rendered the data inaccurate.

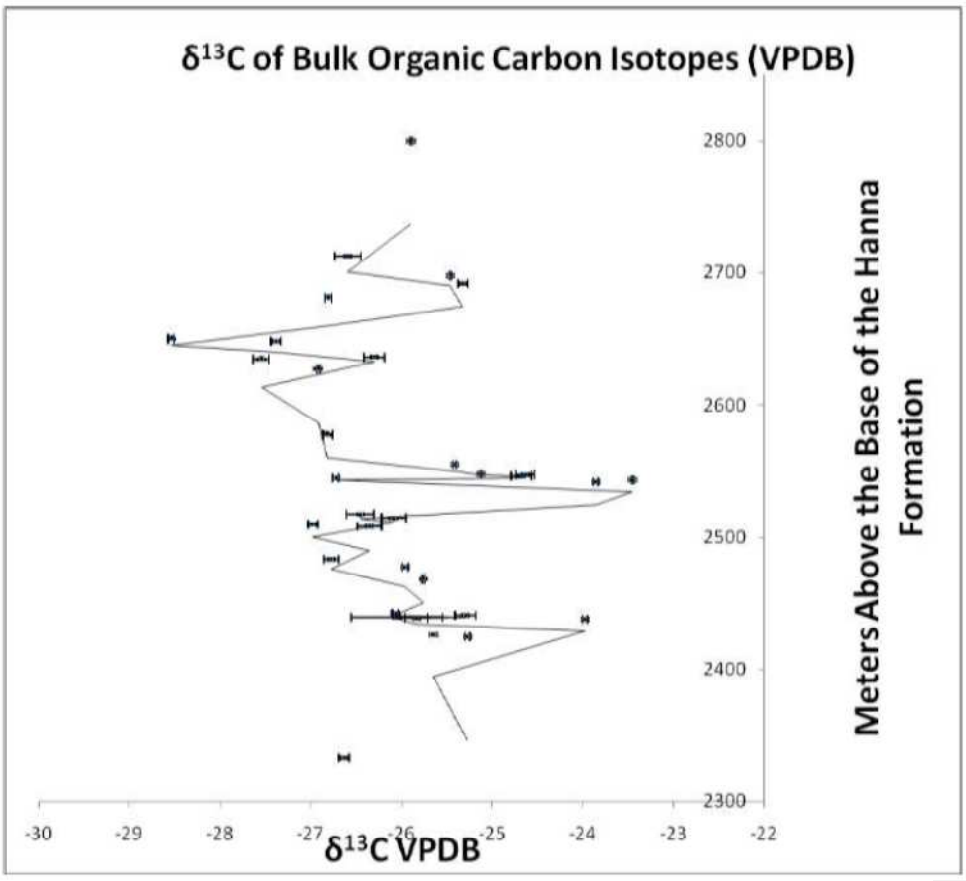

5.2 Results

The bulk organic carbon isotopes analyzed in this study show a median value of approximately -26.30‰ until approximately 2520 meters, then there is an approximately +2‰

shift followed by a -2 ‰ shift between 2550 and 2650 meters above the base of the Hanna Formation followed by a return to a median value of -26.08‰ (see figure 5.1). The negative CIE in the Hanna Formation starts approximately 50 meters above the first occurrence of *P. platycaryoides* and a changed assemblage of pollen which includes many early Eocene morphotypes. This is consistent with previous studies, which have shown that environmental changes may have begun as early as 150 kyrs prior to the CIE, which marks the onset of the PETM (Luciani *et al*., 2007).The presence of the negative carbon isotope excursion nearly concurrent with early Eocene pollen implies that the stratigraphic location of the PETM is between 2600 to 2650 meters above the base of the Hanna Formation.

5.3 Discussion

The bulk organic isotopes analyzed in this study show an approximately +2‰ shift followed by a -2 ‰ shift between 2550 and 2650 meters above the base of the Hanna Formation. This is in accordance with other studies throughout the Western Interior which have also reported 2-4‰ negative CIE's in the PETM interval (Magioncalda *et al*., 2004; Harrington *et al*., 2005). The observed CIE in the Hanna Formation is also commensurate with the CIE observed in marine sections, where a 2-3‰ negative shift in $\delta^{13}C$ values is common at the onset of the PETM (Pagani *et al*., 2006a; Giusberti *et al*., 2007; Koch *et al*., 1992). Since this similar signal is seen in marine and terrestrial systems and appears to be a global phenomenon, the cause of the CIE is not likely the result of local or regional affects such as local floral changes or preservation differences as these would not be ubiquitous across different environments globally. Therefore, the conclusion that the CIE was brought about by an increased flux of isotopically light carbon to the atmosphere is most likely correct. The source of that carbon can only be inferred by making

estimates of the size of the carbon source and the isotopic signature of that source relative to the overall global shift in $\delta^{13}C$ values.

However, the +2‰ shift is an anomaly that does not appear to be present in other PETM sections. There are a number of potential reasons for this shift. It occurs within the fluvial unit, where it is possible that reworked carbon from local uplift and erosion due to Laramide tectonics was incorporated into the transported sediment. $\delta^{13}C$ of bulk marine carbonates decreased on the order of 2‰ during the post K/Pg recovery interval at the start of the Cenozoic, but rebounded to pre-K/Pg levels by the late Paleocene (Corfield, 1994; Zachos *et al*., 2001). If isotopically heavy rocks from the Cretaceous, such as the Ferris Formation spanning the K/Pg boundary or a number of Cretaceous formations found nearby including the Lewis Shale, Mesaverde Group, Steele Shale, Niobrara or Frontier Formations were reworked then this may be a possible explanation for the observed positive CIE prior to the negative CIE in the Hanna Basin section.

Additionally, as the observed positive CIE is only represented by two samples, this could represent a sampling bias or taphonomic anomaly within those two samples, which are located very close stratigraphically. This could be due to environmental changes resulting in preferential preservation of different plant organs. Different plant organs fractionate carbon to slightly different degrees. Leaves tend to have most negative values, while woody parts and roots are more positive. So a switch to more root and wood preservation may be the cause of this observed positive CIE.

Another potential source of change may have to do with carbon cycling dynamics in forest understories. In a forest understory carbon has a tendency to be reworked leading to carbon isotope ratios that are relative to the carbon isotope ratios in open air environments,

which may more accurately reflect general atmospheric composition. If there was a change in forest structure during this time caused by changes in relative abundance of canopy trees during this time, then this may have had an effect on the average bulk organic carbon signature, however there is no palynological evidence for reworking of Cretaceous sediments.

The CIE does not coincide with the P-E boundary as defined by the first appearance of *P. platycaryoides*. This may be due to the reworking and redeposition of old organic carbon, as discussed above. Older, isotopically heavier sources of carbon may have obscured the actual onset of the CIE, which may have actually occurred earlier in the stratigraphic section. Alternatively, the better stratigraphic resolution in the Hanna Basin may be capturing an actual phenomenon that is obscured in other basins. Additionally, if there was a northward migration of plant species during the PETM it is possible that the geographic location and environment encouraged *P. platycaryoides* to appear earlier in the Hanna Basin than in other more northern Wyoming basins.

The depositional environment in the Hanna Basin appears to have changed during the PETM interval. The fluvial unit extends until approximately 2630 meters above the base of the Hanna Formation, indicating a riverine system existed up until that point. Stratigraphically above the fluvial unit is the upper lacustrine unit, which begins at 2630 meters. The transition between fluvial and lacustrine environment occurs during the interval in which the CIE is found, indicating that a major change in depositional environment occurred contemporaneously with the PETM interval. This phenomenon is observed at other PETM sites and is believed to be the result of climate change affecting regional weather patterns and ecosystems (Schmitz *et al*., 2007; Foreman & Heller, 2009). It is well recorded in the nearby Wind River Basin, where the pre-PETM interval is dominated by mudstones followed by fluvial channel beds occurring just

below the CIE onset. This has been interpreted in the Wind River Basin as a sedimentation change due to climate change prior to the main phase of the PETM, but could also result from the onset of the CIE being obscured by erosion and re-deposition of pre-PETM carbon sources (Rasmussen & Fricke, 2012). Given the somewhat disjunct palynological, isotopic and stratigraphic evidence in the Hanna Basin, the same processes could have obscured the true location of the start of the PETM CIE in the Hanna Formation.

After the positive and negative CIE's observed in the Hanna Basin record the carbon isotope signal appears to return to mean background levels established during the pre-CIE interval. Previous studies have posited that this occurred because of rapid carbon draw down from increased productivity, weathering rates and carbon burial (John, 2008).

Methane hydrate dissociation is the most widely accepted cause for the PETM (Thomas *et al*., 2002). However, there are many alternate theories for the origin of the negative CIE at the onset of the PETM. Taphonomic bias is one potential cause for the CIE. This would occur because the isotopic compositions recorded in different plant organs can differ from one another and can bias isotopic analyses of bulk organic matter. For example, modern woody material has an isotopic ratio of ~-24‰ and non-woody material exhibits values of ~-30‰ (Foster *et al.*, 1997). However, this is not a likely cause of the CIE, because there would have to be a consistent and ubiquitous taphonomic bias globally in both marine and terrestrial sections as the CIE is observed to have a similar magnitude globally, with a slightly larger excursion in marine sections. However, specific studies of plant organs could help to recognize if reworking and redeposition of older organic material is obscuring the magnitude or onset of the CIE in terrestrial sections, particularly where large changes in deposition style occurred during the CIE/ PETM interval such as that in the Hanna Formation.

Other potential causes of the CIE invoke other forms of carbon release to the atmosphere, but ultimately create similar atmospheric and climatic results. These include desiccation of epicontinental seaways, comet impact and biomass burning. However, none of these sources has a sufficient reservoir size or sufficiently negative $\delta^{13}C$ values to be the sole cause for the observed negative CIE during the PETM (Higgins, 2006; Kent *et al*., 2003; Moore & Kurtz, 2008).

Previously, the PETM in the Hanna Formation was constrained to between 2350 and 2800 meters above the local base of the Hanna Formation, based on fresh water mollusks fossils and broad-scale palynological studies (Kirschner *et al*., 1984, Lillegraven *et al*., 2004). In this study, due to the use of both stable isotope and palynological data the PETM has been stratigraphically located more precisely to an approximately 50 meter portion of the section approximately 2600-2650 meters above the base of the Hanna Formation. This is a somewhat thicker boundary section than is observed in other Wyoming P-E basins and thus indicates greater stratigraphic resolution in the Hanna Basin. When coupled to the disjunction between the palynological and isotopic indicators for the P-E boundary and PETM CIE in the Hanna Basin, this demonstrates the potential of this site for follow-up studies to further elucidate the cause and nature of the PETM paleoclimatic event.Late Paleocene mammalian fossils have been used in previous studies to constrain sedimentation rates through the PETM at 0.2-0.3 mm/year (Higgins, 2000, 2003). This coupled with evidence for increased tectonic activity later in basin formation implies that sedimentation rates near the top of the Hanna Formation were even greater than 0.3 mm/year (Lillegraven & Snoke, 1996). Given that the PETM is estimated to have lasted for up to 200,000 years and the estimates of ~0.3 mm/year sedimentation rates, the PETM section in the Hanna Basin would be expected to be approximately 60 meters. This

expected thickness is commensurate with the interval in which this study has found the -2 ‰ CIE and subsequent return to near background levels.

5. 4 Conclusion

This study has succeeded in more precisely determining the PETM interval and the CIE in the Hanna Formation of the Hanna Basin, WY. Previous work constrained the PETM interval to between 2350-2800 meters above the base of the Hanna Formation. This study has constrained the CIE to 2600-2650 meters and the PETM interval (initiation to return to background) from approximately 2600-2750 meters. This implies that the PETM interval in the Hanna Basin extends approximately 150 meters, which offers the potential for substantially greater sampling resolution than in other Wyoming sections, such as one found in Bighorn Basin, which is restricted to only 40 meters (Wing *et al*., 2003). The determination of a more precise location for the PETM in the Hanna Basin has paved the way for additional future work to provide more insight into paleocological and environmental changes during the PETM in the Hanna Basin.

Chapter 6 General Conclusions

Results show an approximately -2 ‰ shift in organic carbon isotopic signature between approximately 2600-2650 meters above the base of the Hanna Formation. *Platycarya* pollen first occurs just down section of the observed CIE in organic carbon, first appearing at 2540 meters above the base of the section. The first occurrence of *Platycarya platycaryoides* along with the observed carbon isotope excursion suggests that the onset of the PETM and P-E Boundary in the Hanna Basin are located at between 2540 and 2650 meters. Thus, this study succeeded in more precisely locating the PETM with in the Hanna Formation.

The disjunction between the isotopic and palynological indicators of the P-E boundary and PETM CIE in the Hanna Basin is unique regionally. This phenomenon may result from earlier immigration of *Platycarya* in to the basin because of its more southerly location, reworked isotopically heavy organic carbon from underlying Cretaceous rocks obscuring the start of the negative CIE, a change in the plant organs contributing to the bulk organic carbon isotopic signatures, or perhaps the greater stratigraphic resolution in the Hanna Basin reveals a feature that is widespread but cryptic in other basins. If the latter, then the biotic changes accompanying the P-E boundary preceded the main paleoclimatic event, which would have profound implications for our predictions of the consequences of modern climate change.

Continued study is necessary to rule out taphonomic bias as a potential cause for the CIE. This could occur because the isotopic compositions recorded in different plant organs can differ from one another and can bias isotopic analyses of bulk organic matter. For example, modern woody material has an isotopic ratio of ~-24‰ and non-woody material exhibits values of ~-30‰ (Foster *et al*, 1997). Therefore, if the relative amount of different plant organs varies

between samples across the Paleocene-Eocene (P-E) boundary, this would obscure the true magnitude and stratigraphic location of the CIE, based on bulk organic carbon $\delta^{13}C$ values.

Now that the stratigraphic location of the CIE and thus the onset of the PETM have been determined, further work should be done to characterize how this major climate event impacted local and regional plant assemblages and ecology. Further palynological study should be done in order to look more closely at the recovery interval in order to determine how plant communities behaved during recovery. In particular, there are numerous leaf macrofossils, many containing intact cuticles, which could also be used in future studies of floral change in the Hanna Basin, with the aim of constraining changing atmospheric pCO_2 across this interval. Stomate size and abundance in leaf cuticle can be a good proxy for pCO_2 if control studies under varying pCO_2 are conducted using nearest living relatives (Doria *et al*., 2011).

Additional studies should also be conducted to better characterize facies changes across the PETM as the onset of the CIE appears to be coincident with a major facies shift from fluvial to lacustrine. This facies shift may be indicative of local or regional precipitation and weather changes due to this major climate event which may in turn have affected floral communities thus modifying the isotopic signature of the event.

In order to determine what were the factors behind the floral changes in the Hanna Basin paleoaltitudinal studies should also be conducted. This would show whether changes in altitude contributed to or lessened the impacts of regional climate change during the PETM. Such studies could perhaps use oxygen isotopes or clumped isotopes in pedogenic carbonates, as these vary with altitude (Peters *et al*., 2010). Clumped isotopes can also be used potentially to more directly calculate paleotemperatures as clumped isotopes do not require assumptions about the $d^{18}O$ of

the water in which carbonates formed in order to calculate temperature. The abundance of fresh water molluscs provide a source of carbonate material which could be used for clumped isotope studies in the Hanna Basin section.

Further studies as suggested above will help to build upon the work of this thesis in order to determine more quantitatively what the local and regional scale paleoecological and paleoenvironmental impacts of this major climate event were. This thesis shows that the Hanna Basin section evidently has greater stratigraphic resolution and a more complex P-E boundary and PETM scenario and other basins in the region and therefore offers an apparently unmatched window into the effects of sudden climate change upon biotic communities.

Acknowledgements

Roger Buick, Linda Reinink-Smith, Regan Dunn, Caroline Stromberg, Pennilyn Higgins, Estella Leopold, Jay and Linda Lillegraven, Kay Lynn and Burt Palm, Rick and Tad Dilhoff, Geological Society of America Graduate Research Grant, Paleontological Society, Colorado Scientific Society, NSF OACIS GK-12, Washington NASA Space Grant, University of Washington Earth and Space Sciences Department, Goodspeed Research Grant, Vance Research Scholarship, and Bourgeois Research Grant.

REFERENCES CITED

Agnini C, Fornaciari E, Rio D, Tateo F, Backman J, Giusberti L. 2007. Responses of calcareous nannofossil assemblages, mineralogy and geochemistry to the environmental perturbations across the Paleocene/Eocene boundary in the Venetian Pre-Alps. Mar. Micropaleontol. 63:19–38

Alegret L, Ortiz S, Molina E. 2009a. Extinction and recovery of benthic foraminifera across the Paleocene Eocene Thermal Maximum at the Alamedilla section (Southern Spain). Palaeogeogr. Palaeoclimatol.Palaeoecol. 279:186–200

Alegret L, Ortiz S, Orue-Etxebarria X, Bernaola G, Baceta JI, et al. 2009b. The Paleocene-Eocene thermal maximum: new data on microfossil turnover at the Zumaia section, Spain. Palaios 25:318–28

Angori E, Bernaola G, Monechi S. 2007. Calcareous nannofossil assemblages and their response to the Paleocene-Eocene Thermal Maximum event at different latitudes: ODP Site 690 and Tethyan sections. Geol. Soc. Am. Spec. Pap. 424:69–85

Aziz HA, Hilgen FJ, van Luijk GM, Sluijs A, Kraus MJ, et al. 2008. Astronomical climate control on paleosol stacking patterns in the upper Paleocene-lower EoceneWillwood Formation, Bighorn Basin,Wyoming. Geology 36:531–34

Bains S, Corfield RM, Norris RD. 1999. Mechanisms of climate warming at the end of the paleocene. Science 285(5428; 5428):724-7.

Bains S, Norris RD, Corfield RM, Bowen GJ, Gingerich PD, Koch PL. 2003. Marine-terrestrial linkages at the paleocene-eocene boundary. Special Paper - Geological Society of America 369:1-9.

Boucsein B, Stein R. 2009. Black shale formation in the late Paleocene/early Eocene Arctic Ocean and paleoenvironmental conditions: new results from a detailed organic petrological study. Mar. Petroleum Geol. 26:416–26

Bourque J, Hutchison JH, Holroyd P, Bloch JI. 2008. A new kinosternoid (Testudines: Dermatemydidae) from thePaleocene-Eocene boundary of the Bighorn Basin, Wyoming, and its paleoclimatological implications. J. Vertebr. Paleontol. 28(3):55A

Bowen GJ, Koch PL, Gingerich PD, Norris RD, Bains S, Corfield R. 2001. Refined isotope stratigraphy across the continental Paleocene-Eocene boundary on Polecat Bench in the northern Bighorn Basin. Univ. Mich. Pap. Paleontol. 33:73–88

Bowen GJ, Koch PL, Meng J, Ye J, Ting SY. 2005. Age and correlation of fossiliferous late Paleocene-early eocene strata of the Erlian basin, Inner Mongolia, China. Am. Mus. Novit. 3474:1–26

Bowen GJ, Zachos JC. 2010. Rapid carbon sequestration at the termination of the Palaeocene-EoceneThermal Maximum. Nat. Geosci. 3:866–69

Bown P, Pearson P. 2009. Calcareous plankton evolution and the Paleocene/Eocene thermal maximum event: new evidence from Tanzania. Mar. Micropaleontol. 71:60–70

Boyd DW and Lillegraven JA. 2011. Persistence of the western interior seaway; historical background and significance of ichnogenus rhizocorallium in paleocene strata, south-central wyoming. Rocky Mountain Geology 46(1; 1):43-69.

Bralower TJ. 2002. Evidence of surface water oligotrophy during the Paleocene-Eocene thermal maximum: nannofossil assemblage data from Ocean Drilling Program Site 690, Maud Rise, Weddell Sea.

Chamberlain CP, Mix HT, Mulch A, Hren MT, Kent-Corson M, Davis SJ, Horton TW, Graham SA. 2012. The cenozoic climatic and topographic evolution of the western north american cordillera. Am J Sci 312(2; 2):213-62.

Chester S, Bloch J, Secord R, Boyer D. 2010. A new small-bodied species of Palaeonictis (Creodonta, Oxyaenidae) from the Paleocene-Eocene Thermal Maximum. J. Mamm. Evol. 17:227–43

Clechenko ER, Kelly DC, Stiles CA, Harrington GJ, Valley JW. 2005. Enhanced continental weathering and pedogenesis across the Paleocene/Eocene boundary in the U.S. western interior (north dakota). Abstracts with Programs - Geological Society of America 37(7; 7):265-.

Clyde WC, Gingerich PD. 1998. Mammalian community response to the Latest Paleocene Thermal Maximum: an isotaphonomic study in the northern Bighorn Basin, Wyoming. Geology 26:1011–14

Corfield RM. 1994.Palaeocene oceans and climate; an isotopic perspective. Earth-Sci Rev 37(3-4; 3-4):225-52.

Cramer BS and Kent DV. 2005. Bolide summer; the Paleocene/Eocene thermal maximum as a response to an extraterrestrial trigger. Palaeogeogr , Palaeoclimatol , Palaeoecol 224(1-3; 1-3):144-66.

Crouch EM, Dickens GR, Brinkhuis H, Aubry M, Hollis CJ, Rogers KM, Visscher H. 2003. The apectodinium acme and terrestrial discharge during the paleocene-eocene thermal maximum; new palynological, geochemical and calcareous nannoplankton observations at tawanui, new zealand. Palaeogeogr , Palaeoclimatol , Palaeoecol 194(4; 4):387-403.

Crouch EM, Heilmann-ClausenC,Brinkhuis H, MorgansHEG,RogersKM,et al. 2001. Global dinoflagellate event associated with the Late Paleocene Thermal Maximum. Geology 29:315–18

Currano ED, Wilf P, Wing SL, Labandeira CC, Lovelock EC, Royer DL. 2008. Sharply increased insect herbivory during the paleocene-eocene thermal maximum. Proc Natl Acad Sci U S A 105(6; 6):1960-4.

DeConto R, Galeotti S, Pagani M, Tracy DM, Pollard D, Beerling DJ. 2010. Hyperthermals and orbitally paced permafrost soil organic carbon dynamics. Presented at AGU Fall Meet., Dec. 13–17, San Francisco (Abstr. PP21E-08)

Dickens GR, Castillo MM, Walker JCG. 1997. A blast of gas in the latest paleocene; simulating first-order effects of massive dissociation of oceanic methane hydrate. Geology [Boulder] 25(3; 3):259-62.

Dickens GR, O'Neil JR, Rea DK, Owen RM. 1995. Dissociation of oceanic methane hydrate as a cause of the carbon isotope excursion at the end of the paleocene. Paleoceanography 10(6; 6):965-71.

Dickinson WR. 2003. The basin and range province as a composite extensional domain. International Book Series 7:213,250@3sheets.

Dickinson WR. 2003. The basin and range province as a composite extensional domain. International Book Series 7:213,250@3sheets.

Diefendorf AF, Mueller KE, Wing SL, Koch PL, Freeman KH. 2010. Global patterns in leaf 13C discrimination and implications for studies of past and future climate. Proc. Natl. Acad. Sci. USA 107:5738–43

Doher LI. 1980.Palynomorph preparation procedures currently used in the paleontology and stratigraphy laboratories, U. S. geological survey. United States: U. S. Geological Survey : Reston, VA, United States.

Dostal J, Keppie JD, Church BN, Reynolds PH, Reid CR. 2008. The eocene-oligocene magmatic hiatus in the south-central canadian cordillera; a capture of the kula plate by the pacific plate? Canadian Journal of Earth Sciences = Revue Canadienne Des Sciences De La Terre 45(1; 1):69-82.

DREW C and TSCHUDY B. 1968. Aquilapollenites - fossil pollen as seen under scanning electron microscope. Geol Soc Am Bull 79(12):1829,&.

Foster DA and Fanning CM. 1997. Geochronology of the northern idaho batholith and the bitterroot metamorphic core complex; magmatism preceding and contemporaneous with extension. Geological Society of America Bulletin 109(4; 4):379-94.

Fricke HC, Clyde WC, O'Neil JR, Gingerich PD. 1998. Evidence for rapid climate change in north america during the latest paleocene thermal maximum; oxygen isotope compositions of biogenic phosphate from the bighorn basin (wyoming). Earth Planet Sci Lett 160(1-2; 1-2):193-208.

Fricke HC, Wing SL. 2004. Oxygen isotope and paleobotanical estimates of temperature and δ18O-latitude gradients over North America during the early Eocene. Am. J. Sci. 304:612–35

Fuentes F, DeCelles PG, Constenius KN. 2012. Regional structure and kinematic history of the cordilleran fold-thrust belt in northwestern montana, USA. Geosphere 8(5; 5):1104-28.

Funkhouser JW and Evitt,William Robert,,II. 1959. Preparation techniques for acid-insoluble microfossils. Micropaleontology 5(3; 3):369-75.

Gavrilov YO, Shcherbinina EA, Oberh¨ansli H. 2003. Paleocene-Eocene boundary events in the northeastern Peri-Tethys. Geol. Soc. Am. Spec. Pap. 369:147–68

Gibbs SJ, Bown PR, Sessa JA, Bralower TJ, Wilson PA. 2006. Nannoplankton extinction and origination across the paleocene-eocene thermal maximum. Science 314(5806; 5806):1770-3.

Gibbs SJ, Bralower TJ, Bown PR, Zachos JC, Bybell LM. 2006. Shelf and open-ocean calcareous phytoplankton assemblages across the paleocene-eocene thermal maximum; implications for global productivity gradients. Geology [Boulder] 34(4; 4):233-6.

Gingerich PD and Gunnell GF. 2005. Brain of plesiadapis cookei (mammalia, proprimates); surface morphology and encephalization compared to those of primates and dermoptera. Contributions from the Museum of Paleontology University of Michigan 31(8; 8):185-95.

Gingerich PD and Smith T. 2006. Paleocene-eocene land mammals from three new latest clarkforkian and earliest wasatchian wash sites at polecat bench in the northern bighorn basin, wyoming. Contributions from the Museum of Paleontology University of Michigan 31(11; 11).

Gingerich PD. 2003. Mammalian responses to climate change at the paleocene-eocene boundary; polecat bench record in the northern bighorn basin, wyoming. Special Paper - Geological Society of America 369:463-78.

Gingerich PD. 2007. Faunal and environmental change across the paleocene-eocene boundary in the north american continental interior; bighorn basin, wyoming. Abstracts with Programs - Geological Society of America 39(6; 6):191-2.

Giusberti L, Rio D, Agnini C, Backman J, Fornaciari E, et al. 2007. Mode and tempo of the Paleocene-Eocene thermal maximum in an expanded section from the Venetian pre-Alps. Geol. Soc. Am. Bull. 119:391–412

Gowik U and Westhoff P. 2011. The path from C-3 to C-4 photosynthesis. Plant Physiol 155(1):56-63.

Hanley JH and Flores RM. 1987. Taphonomy and paleoecology of nonmarine mollusca; indicators of alluvial plain lacustrine sedimentation, upper part of the tongue river member, fort union formation (paleocene), northern powder river basin, wyoming and montana. Palaios 2(5; 5):479-96.

Harrington GJ and Jaramillo CA. 2007. Paratropical floral extinction in the late palaeocene-early eocene. Journal of the Geological Society of London 164(2; 2):323-32.

Harrington GJ, Clechenko ER, Clay Kelly D. 2005. Palynology and organic-carbon isotope ratios across a terrestrial Palaeocene/Eocene boundary section in the williston basin, north dakota, USA. Palaeogeogr , Palaeoclimatol , Palaeoecol 226(3-4; 3-4):214-32.

Harrington GJ, Kemp SJ, Koch PL. 2004. Palaeocene-eocene paratropical floral change in north america; responses to climate change and plant immigration. Journal of the Geological Society of London 161(2; 2):173-84.

Harrington GJ. 2001. Pollen assemblages and paleocene-eocene stratigraphy in the bighorn and clark's fork basins. Papers on Paleontology 33:89-96.

Harrington GJ. 2001. Pollen assemblages and paleocene-eocene stratigraphy in the bighorn and clark's fork basins. Papers on Paleontology 33:89-96.

Harrington GJ. 2003. Geographic patterns in the floral response to paleocene-eocene warming. Special Paper - Geological Society of America 369:381-93.

Hasiotis ST and Honey JG. 2000. Paleohydrologic and stratigraphic significance of crayfish burrows in continental deposits; examples from several paleocene laramide basins in the rocky mountains. Journal of Sedimentary Research 70(1; 1):127-39.

Higgins JA and Schrag DP. 2006. Beyond methane; towards a theory for the paleocene-eocene thermal maximum. Earth Planet Sci Lett 245(3-4; 3-4):523-37.

Higgins P. 2003. A wyoming succession of paleocene mammal-bearing localities bracketing the boundary between the torrejonian and tiffanian north american land mammal 'ages'. Rocky Mountain Geology 38(2; 2):247-80.

Hildebrand RS. 2007. Was laramide thick-skinned deformation caused by paleocene slab failure in a subducting north american plate? Abstracts with Programs - Geological Society of America 39(6; 6):230-.

Hildebrand RS. 2009. Did westward subduction cause cretaceous-tertiary orogeny in the north american cordillera? Special Paper - Geological Society of America 457.

Holroyd P, Hutchison J, Strait S. 2001. Turtle diversity and abundance through the lower Eocene Willwood Formation of the southern Bighorn Basin. Univ. Mich. Pap. Paleontol. 33:97–107

Hooker JJ. 1998. Mammalian faunal change across the Paleocene-Eocene transition in Europe. See Aubry et al. 1998, pp. 428–50

Huber M and Sloan LC. 1999. Warm climate transitions; a general circulation modeling study of the late paleocene thermal maximum (approximately 56 ma). Journal of Geophysical Research 104:16.

Intergov. Panel Clim. Change (IPCC). 2007. Climate Change 2007: The Physical Science Basis. Contributions of Working Group I to the Fourth Assesment Report of the Intergovernmental Panel on Climate Change. Washington, DC: IPCC

Ivany LC, Sessa JA. 2010. Effects of ocean warming and acidification during the Paleocene-Eocene Thermal Maximum on deep and shallow marine communities. Presented at Ecol. Soc. Am. Annu. Meet., Pittsburgh, PA

Jablonski D. 2001.Lessons from the past; evolutionary impacts of mass extinctions. Proc Natl Acad Sci U S A 98(10; 10):5393-8.

Jacobs DK and Lindberg DR. 1998.Oxygen and evolutionary patterns in the sea; onshore/offshore trends and recent recruitment of deep-sea faunas. Proc Natl Acad Sci U S A 96(16; 16):9396-401.

Jaramillo CA,Ochoa D, Contreras L, PaganiM, Carvajal-OrtizH, et al. 2010. Effects of rapid global warming at the Paleocene-Eocene boundary on Neotropical vegetation. Science 330:957–61

Johnson KR. 2002. Early paleocene landscapes of the rocky mountain region. Abstracts with Programs - Geological Society of America 34(1; 1):62-.

KaihoK,Arinobu T, IshiwatariR,MorgansHEG,OkadaH, et al. 1996. Latest Paleocene benthic foraminiferal extinction and environmental changes at Tawanui, New Zealand. Paleoceanography 11:447–65

Katz ME, Cramer BS, Mountain GS, Katz S, Miller KG. 2001. Uncorking the bottle; what triggered the Paleocene/Eocene thermal maximum methane release? Paleoceanography 16(6; 6):549-62.

Katz ME, Pak DK, Dickens GR, Miller KG. 1999. The source and fate of massive carbon input during the Latest Paleocene Thermal Maximum. Science 286:1531–33

Kennett JP and Stott LD. 1991.Abrupt deep-sea warming, palaeoceanographic changes and benthic extinctions at the end of the palaeocene. Nature [London] 353(6341; 6341):225-9.

Kent DV, Cramer BS, Lanci L, Wang D, Wright JD, Van dV. 2003. A case for a comet impact trigger for the Paleocene/Eocene thermal maximum and carbon isotope excursion. Earth Planet Sci Lett 211(1-2; 1-2):13-26.

Kent-Corson M, Sherman LS, Mulch A, Chamberlain CP. 2006. Cenozoic topographic and climatic response to changing tectonic boundary conditions in western north america. Earth Planet Sci Lett 252(3-4; 3-4):453-66.

Kirschner WA. 1984. Nonmarine molluscan paleontology and paleoecology of early tertiary strata, hanna basin, wyoming. United States: .

Koch PL, Clyde WC, Hepple RP, Fogel ML, Wing SL, Zachos JC. 2003. Carbon and oxygen isotope records from paleosols spanning the paleocene-eocene boundary, bighorn basin, wyoming. Special Paper - Geological Society of America 369:49-64.

Koch PL, Zachos JC, Gingerich PD. 1992. Correlation between isotope records in marine and continental carbon reservoirs near the Palaeocene/Eocene boundary. Nature [London] 358(6384; 6384):319-22.

Kraus MJ and Riggins S. 2007. Transient drying during the paleocene-eocene thermal maximum (PETM); analysis of paleosols in the bighorn basin, wyoming. Palaeogeogr , Palaeoclimatol , Palaeoecol 245(3-4; 3-4):444-61.

Kraus MJ, Woody D, Smith J, Hasiotis ST. 2008. Rapid paleoenvironmental change during the paleocene-eocene thermal maximum (PETM), bighorn basin, WY. Abstracts: Annual Meeting - American Association of Petroleum Geologists 2008.

Kurtz AC, Kump LR, Arthur MA, Zachos JC, Paytan A. 2003. Early cenozoic decoupling of the global carbon and sulfur cycles. Paleoceanography 18(4; 4).

Kvenvolden KA. 1993. Gas hydrates—geological perspective and global change. Rev. Geophys. 31:173–87

Kvenvolden KA. 1999. Potential effects of gas hydrate on human welfare. United States: National Academy of Sciences : Washington, DC, United States. Report nr 96. 3420 p. .

Landon SC. 2001. Depositional packages and scales of avulsion in a thick alluvial basin fill, hanna basin, central wyoming. United States: .

Lawrence KT, Sloan LC, Sewall JO. 2003. Terrestrial climatic response to precessional orbital forcing in the eocene. Special Paper - Geological Society of America 369:65-77.

Leffingwell HA and Hodgkin N. 1971.Techniques for preparing fossil palynomorphs for study with the scanning and transmission electron microscopes. Rev Palaeobot Palynol 11(3-4; 3-4):177-99.

Lillegraven JA and Eberle JJ. 1999. Vertebrate faunal changes through lancian and puercan time in southern wyoming. J Paleontol 73(4; 4):691-710.

Lillegraven JA, Snoke AW, McKenna MC. 2004. Tectonic and paleogeographic implications of late laramide geologic history in the northeastern corner of wyoming's hanna basin. Rocky Mountain Geology 39(1; 1):7-64.

Lillegraven JA[and Snoke AW[. 1996. A new look at the laramide orogeny in the seminoe and shirley mountains, freezeout hills, and hanna basin, south-central wyoming. United States: Geological Survey of Wyoming : Laramie, WY, United States.

Luciani V, Giusberti L, Agnini C, Backman J, Fornaciari E, Rio D. 2007. The paleocene-eocene thermal maximum as recorded by tethyan planktonic foraminifera in the forada section (northern italy). Mar Micropaleontol 64(3-4; 3-4):189-214.

Luciani V, Giusberti L, Agnini C, Backman J, Fornaciari E, Rio D. 2007. The paleocene-eocene thermal maximum as recorded by tethyan planktonic foraminifera in the forada section (northern italy). Mar Micropaleontol 64(3-4; 3-4):189-214.

Luciani V, Giusberti L, Agnini C, Backman J, Fornaciari E, Rio D. 2007. The paleocene-eocene thermal maximum as recorded by tethyan planktonic foraminifera in the forada section (northern italy). Mar Micropaleontol 64(3-4; 3-4):189-214.

Luterbacher H, Hardenbol J, Schmitz B. 2000. Decision of the voting members of the International Subcommission on Paleogene Stratigraphy on the criterion for the recognition of the Paleocene/Eocene boundary. Newsl. Int. Subcomm. Paleogene Stratigr. 9:13

Magioncalda R, Dupuis C, Smith T, Steurbaut E, Gingerich PD. 2004. Paleocene-eocene carbon isotope excursion in organic carbon and pedogenic carbonate; direct comparison in a continental stratigraphic section. Geology [Boulder] 32(7; 7):553-6.

Matell N, Theberge A, Stoll HM, Shimuzu N. 2005. Tropical atlantic coccolith Sr/Ca productivity records from the paleocene-eocene thermal maximum. Abstracts with Programs - Geological Society of America 37(1; 1):76-.

Mitchell JH. 2002. Sedimentary record of late cretaceous through paleocene evolution of the bighorn basin, wyoming. United States: .

Moore EA and Kurtz AC. 2008.Black carbon in paleocene-eocene boundary sediments; a test of biomass combustion as the PETM trigger.Palaeogeogr , Palaeoclimatol , Palaeoecol 267(1-2; 1-2):147-52.

Morsi AM, Speijer RP, Stassen P, Steurbaut E. 2011. Shallow marine ostracode turnover in response to environmental change during the Paleocene-Eocene thermal maximum in northwest Tunisia. J. Afr. Earth Sci. 59:243–68

Mutterlose J, Linnert C, Norris R. 2007. Calcareous nannofossils from the Paleocene-Eocene thermal maximum of the equatorial Atlantic (ODP Site 1260B): evidence for tropical warming. Mar. Micropaleontol. 65:13–31

Nichols DJ and Ott HL. 1978. Biostratigraphy and evolution of the momipites-caryapollenites lineage in the early tertiary in the wind river basin, wyoming. Palynology 2:93-112.

O'Leary M. 1981. Carbon isotope fractionation in plants. Phytochemistry 20(4):553-67.

Pagani M, Caldeira K, Archer D, Zachos JC. 2006. An ancient carbon mystery. Science 314(5805; 5805):1556-7.

Pagani M, Pedentchouk N, Huber M, Sluijs A, Schouten S, Brinkhuis H, Sinninghe Damste JS, Dickens GR, Backman J, Clemens S, et al. 2006. Arctic hydrology during global warming at the Palaeocene/Eocene thermal maximum. Nature [London] 442(7103; 7103):671-5.

Panchuk K, Ridgwell A, Kump LR. 2008. Sedimentary response to Paleocene-Eocene Thermal Maximum carbon release: a model-data comparison. Geology 36:315–18

Pocknall DT. 1987. Palynomorph biozones for the fort union and wasatch formations (upper paleocene-lower eocene), powder river basin, wyoming and montana, U.S.A. Palynology 11:23-35.

Rasmussen D and Fricke H. 2012. Possible link between PETM climate change and sedimentological change in the wind river basin, wyoming. Abstracts with Programs - Geological Society of America 44(6; 6):6-.

Raup DM and Sepkoski JJ. 1982. Mass extinctions in the marine fossil record. Science 215(4539; 4539):1501-3.

Roehl U, Westerhold T, Bralower TJ, Zachos JC. 2007. On the duration of the paleocene-eocene thermal maximum (PETM). Geochemistry, Geophysics, Geosystems - G [Super 3] 8(12; 12).

Schmitz B and Pujalte V. 2007.Abrupt increase in seasonal extreme precipitation at the paleocene-eocene boundary. Geology [Boulder] 35(3; 3):215-8.

Schmitz B, Thompson EI, Bornmalm L, Heilmann-Clausen C. 2003. A paleoenvironmental reconstruction of the early late paleocene north sea from intrashell delta (super 18) O and delta (super 13) C profiles of mollusks. Special Paper - Geological Society of America 369:263-74.

Schouten S, Woltering M, Rijpstra WIC, Sluijs A, Brinkhuis H, Damste JSS. 2007. The Paleocene-Eocene carbon isotope excursion in higher plant organic matter: differential fractionation of angiosperms and conifers in the Arctic. Earth Planet. Sci. Lett. 258:581–92

Secord R, Bloch JI, Chester SGB, Boyer DM, Wood AR, Wing SL, Kraus MJ, McInerney FA, Krigbaum J. 2012. Evolution of the earliest horses driven by climate change in the paleocene-eocene thermal maximum. Science 335(6071; 6071):959-62.

Shullenberger ED. 2007. Stratigraphic and mineralogic evidence of paleoweathering at the paleocene-eocene boundary, williston basin, north dakota. United States: .

Sluijs A, Schouten S, Pagani M, WolteringM, Brinkhuis H, et al. 2006. Subtropical Arctic Ocean temperatures during the Palaeocene/Eocene Thermal Maximum. Nature 441:610–13

Smith FA, Wing SL, Freeman KH. 2007. Magnitude of the carbon isotope excursion at the paleocene-eocene thermal maximum; the role of plant community change. Earth Planet Sci Lett 262(1-2; 1-2):50-65.

Smith JJ, Hasiotis ST, Kraus MJ, Woody DT. 2008. Relationship of floodplain ichnocoenoses to paleopedology, paleohydrology, and paleoclimate in the willwood formation, wyoming, during the paleocene-eocene thermal maximum. Palaios 23(10; 10):683-99.

Smith JJ, Hasiotis ST, Kraus MJ,Woody DT. 2009. Transient dwarfism of soil fauna during the Paleocene- Eocene Thermal Maximum. Proc. Natl. Acad. Sci. USA 106:17655–60

Smith KT. 2009. A new lizard assemblage from the earliest Eocene (Zone Wa0) of the Bighorn Basin, Wyoming,USA: biogeography during the warmest interval of the Cenozoic. J. Syst. Palaeontol. 7:299–358

Speelman EN, Sewall JO, Noone D, Huber M, von dH, Sinninghe Damste J, Reichart G. 2010. Modeling the influence of a reduced equator-to-pole sea surface temperature gradient on the distribution of water isotopes in the early/middle eocene. Earth Planet Sci Lett 298(1-2; 1-2):57-65.

Steineck PL, Thomas E. 1996. The latest Paleocene crisis in the deep sea: Ostracode succession at Maud Rise, Southern Ocean. Geology 24:583–86

Stoll HM and Bains S. 2003. Coccolith Sr/Ca records of productivity during the paleocene-eocene thermal maximum from the weddell sea. Paleoceanography 18(2; 2).

Storey M, Duncan RA, Swisher,Carl C., I.,II. 2007. Paleocene-eocene thermal maximum and the opening of the northeast atlantic. Science 316(5824; 5824):587-9.

Strait SG. 2001. NewWa0 mammalian fauna from Castle Gardens in the southeastern Bighorn Basin. Univ. Mich. Pap. Paleontol. 33:127–43

Svensen H, Planke S, Corfu F. 2010. Zircon dating ties NE Atlantic sill emplacement to initial Eocene global warming. J. Geol. Soc. 167:433–36

Svensen H, Planke S, Malthe-Sorenssen A, Jamtveit B, Myklebust R, et al. 2004. Release of methane from a volcanic basin as a mechanism for initial Eocene global warming. Nature 429:542–45

Thermal Maximum on deep-ocean microbenthic community structure: using rank-abundance curves to quantify paleoecological response. Geology 37:783–86

Thomas DJ, Zachos JC, Bralower TJ, Thomas E, Bohaty S. 2002. Warming the fuel for the fire; evidence for the thermal dissociation of methane hydrate during the paleocene-eocene thermal maximum. Geology [Boulder] 30(12; 12):1067-70.

Thomas E and Zachos JC. 1999. Deep-sea faunas during the late paleocene-early eocene climate optimum; boredom or boredom with short periods of terror? Abstracts with Programs - Geological Society of America 31(7; 7):122-.

Thomas E, Shackleton NJ. 1996. The Paleocene-Eocene benthic foraminiferal extinction and stable isotope anomalies. In Correlation of the Early Paleogene in Northwest Europe Correlation of the Early Paleogene in Northwest Europe, Spec. Pub. 101, ed. RWOB Knox, R Corfield, RE Dunay, pp. 401–41. Washington, DC: Geol. Soc.

Thomas E. 1989. Development of Cenozoic deep-sea benthic foraminiferal faunas in Antarctic waters. Geol. Soc. Lond. Spec. Publ. 47:283–96

Van Sickel WA, Kominz MA, Miller KG, Browning JV. 2004. Late cretaceous and cenozoic sea-level estimates; backstripping analysis of borehole data, onshore new jersey. Basin Research 16(4; 4):451-65.

Walther C, Flueh E, Ranero C, von Huene R, Strauch W. 2000. Crustal structure across the pacific margin of nicaragua: Evidence for ophiolitic basement and a shallow mantle sliver. Geophys J Int 141(3):759-77.

Webb AE, Leighton LR, Schellenberg SA, Landau EA, Thomas E. 2009. Impact of the Paleocene-Eocene

Westerhold T, Rohl U, McCarrenHK, Zachos JC. 2009. Latest on the absolute age of the Paleocene-Eocene Thermal Maximum (PETM): new insights from exact stratigraphic position of key ash layers +19 and −17. Earth Planet. Sci. Lett. 287:412–19

Wilf P. 2000. Late paleocene-early eocene climate changes in southwestern wyoming; paleobotanical analysis. Geological Society of America Bulletin 112(2; 2):292-307.

Willis GC. 1999. The utah thrust system; an overview. Utah Geological Association Publication 27:1-10.

Wilson L and Webster R. 1946. Plant microfossils from a fort union coal of montana. Am J Bot 33(4):271-8.

Wing SL, Bloch JI, Bowen GJ, Boyer DM, Chester S, et al. 2009. Coordinated sedimentary and biotic change during the Paleocene-Eocene Thermal Maximum in the Bighorn Basin, Wyoming, USA. Proc. Climat.

Wing SL, Harrington GJ, Bowen GJ, Koch PL. 2003. Floral change during the initial eocene thermal maximum in the powder river basin, wyoming. Special Paper - Geological Society of America 369:425-40.

Wing SL, Harrington GJ, Smith FA, Bloch JI, Boyer DM, Freeman KH. 2005. Transient floral change and rapid global warming at the paleocene-eocene boundary. Science 310(5750; 5750):993-6.

Wing SL, Harrington GJ. 2001. Floral response to rapid warming in the earliest Eocene and implications for concurrent faunal change. Paleobiology 27:539–63

Wing SL. 1998. Late Paleocene-Early Eocene floral and climatic change in the Bighorn Basin, Wyoming. See Aubry et al. 1998, pp. 380–400

Woody DT, Kraus MJ, Smith JJ, Hasiotis ST. 2007. Abrupt paleoenvironmental change during the paleocene-eocene thermal maximum in the bighorn basin, wyoming. Abstracts with Programs - Geological Society of America 39(6; 6):192-.

Wroblewski AFJ. 2000. Tectonic redirection of paleocene fluvial systems, lower hanna formation, southern wyoming. Abstracts with Programs - Geological Society of America 32(7; 7):306-.

Wroblewski AFJ. 2004. New selachian paleofaunas from 'fluvial' deposits of the ferris and lower hanna formations (maastrichtian-selandian, 66-58 ma), southern wyoming. Palaios 19(3; 3):249-58.

Wroblewski AFJ. 2005. Linking climate with laramide tectonism, valley incision, and sedimentary fill; new insights from upper cretaceous and paleocene examples. Abstracts: Annual Meeting - American Association of Petroleum Geologists 14:A156-.

Wroblewski AFJ. 2008. Paleoenvironmental significance of cretaceous and paleocene psilonichnus in southern wyoming. Palaios 23(6; 6):370-9.

Zachos J, Pagani M, Sloan L, Thomas E, Billups K. 2001. Trends, rhythms, and aberrations in global climate 65 Ma to present. Science 292:686–93

Zachos JC, Lohmann KC, Walker JCG, Wise SW. 1993.Abrupt climate changes and transient climates during the paleogene; a marine perspective. J Geol 101(2; 2):191-213.

Zachos JC, Rohl U, Schellenberg SA, Sluijs A, Hodell DA, et al. 2005. Rapid acidification of the ocean during the Paleocene-Eocene Thermal Maximum. Science 308:1611–15

Zachos JC, Schouten S, Bohaty S, Quattlebaum T, Sluijs A, et al. 2006. Extreme warming of mid-latitudecoastal ocean during the Paleocene-Eocene Thermal Maximum: inferences from TEX86 and isotope data. Geology 34:737–40

Zachos JC,WaraMW, Bohaty S, Delaney ML, Petrizzo MR, et al. 2003. A transient rise in tropical sea surface temperature during the Paleocene-Eocene Thermal Maximum. Science 302:1551–54

Zeebe RE, Zachos JC, Dickens GR. 2009. Carbon dioxide forcing alone insufficient to explain palaeocene-eocene thermal maximum warming. Nature Geoscience 2(8; 8):576-80.